European Commission

ERM
European Reference Materials

CERTIFICATION REPORT

The certification of equivalent diameters of silica nanoparticles in aqueous solution: ERM®-FD101b

EUR 28362 EN - 2017

European Commission
Joint Research Centre
Directorate F – Health, Consumers and Reference Materials

Contact information
Reference materials sales
Address: Retieseweg 111, 2440 Geel, Belgium
E-mail: jrc-rm-distribution@ec.europa.eu
Tel.: +32 (0)14 571 705

JRC Science Hub
https://ec.europa.eu/jrc

JRC105046

EUR 28362 EN

ISBN 978-92-79-64637-9 (PDF)
ISSN 1831-9424 (online)
doi: 10.2787/212519

Luxembourg: Publications Office of the European Union, 2017

Printed in Belgium

Abstract

This report describes the production of ERM®-FD101b, silica nanoparticles suspended in an aqueous solution, certified for different equivalent particle diameters. The material was produced following ISO Guide 34:2009.
The certified reference material (CRM) was produced by the Directorate F - Health, Consumers and Reference Materials of the European Commission's Joint Research Centre (JRC) in Geel (Belgium). The CRM was produced from a diluted and pH adjusted commercial colloidal silica slurry.
Between unit-homogeneity was quantified and stability during dispatch and storage were assessed in accordance with ISO Guide 35:2006. The minimum sample intake for the different methods was determined from the results and information provided by the laboratories that participated in the interlaboratory comparison (ILC) exercises of the characterisation study.
The material was characterised for several equivalent particle diameters based on an interlaboratory comparison amongst laboratories of demonstrated competence and adhering to ISO/IEC 17025. Technically invalid results were removed but no outlier was eliminated on statistical grounds only.
Uncertainties of the certified values were calculated in accordance with the Guide to the Expression of Uncertainty in Measurement (GUM) and include uncertainty contributions related to possible inhomogeneity and instability and to characterisation.
The material is intended for quality control and assessment of method performance. The method-defined certified values are regarded as reliable estimates of the true values and ERM-FD101b can therefore be used for calibration purposes. The CRM is available in 10 mL pre-scored amber glass ampoules each containing about 9 mL of suspension.
The CRM was accepted as European Reference Material (ERM®) after peer evaluation by the partners of the European Reference Materials consortium.

The certification of equivalent diameters of silica nanoparticles in aqueous solution: ERM®-FD101b

Y. Ramaye, V. Kestens, A. Braun, T. Linsinger, A. Held, G. Roebben

European Commission, Joint Research Centre
Directorate F – Health, Consumers and Reference Materials
Geel, Belgium

Disclaimer

Certain commercial equipment, instruments, and materials are identified in this paper to specify adequately the experimental procedure. In no case does such identification imply recommendation or endorsement by the European Commission, nor does it imply that the material or equipment is necessarily the best available for the purpose.

Summary

This report describes the production of ERM®-FD101b, silica nanoparticles suspended in an aqueous solution, certified for different equivalent particle diameters. The material was produced following ISO Guide 34:2009 [1].

The certified reference material (CRM) was produced by the Directorate F - Health, Consumers and Reference Materials of the European Commission's Joint Research Centre (JRC) in Geel (Belgium). The CRM was produced from a diluted and pH adjusted commercial colloidal silica slurry.

Between unit-homogeneity was quantified and stability during dispatch and storage were assessed in accordance with ISO Guide 35:2006 [2]. The minimum sample intake for the different methods was determined from the results and information provided by the laboratories that participated in the interlaboratory comparison (ILC) exercises of the characterisation study.

The material was characterised for several equivalent particle diameters based on an interlaboratory comparison amongst laboratories of demonstrated competence and adhering to ISO/IEC 17025 [3]. Technically invalid results were removed but no outlier was eliminated on statistical grounds only.

Uncertainties of the certified values were calculated in accordance with the Guide to the Expression of Uncertainty in Measurement (GUM) [4] and include uncertainty contributions related to possible inhomogeneity and instability and to characterisation.

The material is intended for quality control and assessment of method performance. The method-defined certified values are regarded as reliable estimates of the true values and ERM-FD101b can therefore be used for calibration purposes. The CRM is available in 10 mL pre-scored amber glass ampoules each containing about 9 mL of suspension.

The CRM was accepted as European Reference Material (ERM®) after peer evaluation by the partners of the European Reference Materials consortium.

The following certified values were assigned:

SILICA NANOPARTICLES IN AQUEOUS SOLUTION			
	Size distribution parameter: Weighting / Averaging	Certified value [7] [nm]	Uncertainty [8] [nm]
Hydrodynamic diameter from DLS [1] (cumulants method)	Scattered light intensity-weighted / harmonic mean	89.5	2.3
Hydrodynamic diameter from DLS [2] (distribution calculation algorithms)	Scattered light intensity-weighted / mean (arithmetic, harmonic, geometric) and modal	93	4
Hydrodynamic diameter from PTA [3]	Number-weighted / modal	82	4
	Number-weighted / arithmetic mean	87	4
	Number-weighted / median	82	4
Stokes diameter from CLS [4] (turbidimetry)	Light extinction-weighted / modal	87	8
Area-equivalent diameter from EM [5]	Number-weighted / modal	83.7	2.2
	Number-weighted / median	83.5	2.2
Mean particle diameter from SAXS [6] (model fitting)	Scattered X-ray intensity-weighted / modal	82.5	1.8
	Volume-weighted / modal	81.7	1.8
	Number-weighted / modal	80.9	1.7

[1] As obtained with dynamic light scattering (DLS) according to ISO 22412:2008 applying the cumulants method described in ISO 13321:1996 at a sample temperature of 25 °C.

[2] As obtained with dynamic light scattering (DLS) applying distribution calculation algorithms such as non-negative least square (NNLS) and CONTIN for data analysis, using various averaging approaches and a sample temperature of 25 °C.

[3] As obtained with particle tracking analysis (PTA) according to ISO 19430:2016 at a sample temperature of 25 °C.

[4] As obtained with centrifugal liquid sedimentation (CLS) according to ISO 13318-1:2001, using an effective particle density of 2.0 g/cm^3 at sample temperatures between 25 °C and 36 °C.

[5] As obtained with transmission and scanning electron microscopy (EM), counting only particles with an equivalent diameter larger than 60 nm.

[6] As obtained with small-angle X-ray scattering (SAXS) according to ISO 17867:2015 at sample temperatures between 23 °C and 25 °C, using 'model fitting' assuming homogeneous spheres and a Gaussian size distribution.

[7] Unweighted mean value of the means of accepted sets of data; each set being obtained in a different laboratory and/or with a different method of determination. The certified value and its uncertainty are traceable to the International System of Units (SI).

[8] The uncertainty of the certified value is the expanded uncertainty with a coverage factor $k = 2$ corresponding to a level of confidence of about 95 % estimated in accordance with ISO/IEC Guide 98-3, Guide to the Expression of Uncertainty in Measurement (GUM:1995), ISO, 2008.

Table of contents

Annexes:

Glossary

AF4	Asymmetrical flow field-flow fractionation
AFM	Atomic force microscopy
ANOVA	Analysis of variance
APD	Avalanche photodiode detector
AUC	Analytical ultracentrifugation
b	Slope of regression line in stability study
CCL	Consultative Committee for Length
CIPM	Comité International des Poids et Mesures (International Committee of Weights and Measures)
CLS	Centrifugal liquid sedimentation
CRM	Certified reference material
D	Diameter of an equivalent sphere
D_{cal}	Assigned diameter of calibrant particles
DLS	Dynamic light scattering
ELS	Electrophoretic light scattering
EM	Electron microscopy
ERM®	Trademark of the European Reference Materials initiative
EU	European Union
GUM	Guide to the Expression of Uncertainty in Measurement
IEC	International Electrotechnical Commission
ILC	Interlaboratory comparison
ISO	International Organization for Standardization
JRC	Joint Research Centre of the European Commission
k	Coverage factor
MALS	Multi-angle light scattering
$MS_{between}$	Mean of squares between-unit from an ANOVA
MS_{within}	Mean of squares within-unit from an ANOVA
n.a.	Not applicable (or not available)
n.c.	Not calculated
n.d.	Not detectable
NNLS	Non-negative least square
p	Number of technically valid datasets
PMT	Photomultiplier tube
PSA	Particle size analysis

PSD	Particle size distribution
PSL	Polystyrene latex
PTA	Particle tracking analysis
PVC	Polyvinyl chloride
q	Scattering vector
QC	Quality control
R	Correlation coefficient
R	Radius of an equivalent sphere
rel	Relative value
R_g	Radius of gyration
R_G	Guinier radius
RI	Refractive index
RM	Reference material
rpm	Revolutions per minute
RSD	Relative standard deviation
s	Standard deviation
SAXS	Small-angle X-ray scattering
s_{bb}	Between-unit standard deviation; an additional index "rel" is added when appropriate
$s_{between}$	Standard deviation between groups as obtained from ANOVA
SE	Secondary electron
SEM	Scanning electron microscopy
SI	International System of Units
s_{within}	Standard deviation within groups as obtained from ANOVA
s_{wb}	Within-unit standard deviation; an additional index "rel" is added when appropriate
$\bar{t}$	Mean of all t_i
t_i	Time elapsed at time point *i*
t_{sl}	Shelf life
t_{tt}	Transport time
TEM	Transmission electron microscopy
TSEM	Transmission-mode scanning electron microscopy
U	Expanded uncertainty; an additional index "rel" is added when appropriate
u	Standard uncertainty; an additional index "rel" is added when appropriate
u^*_{bb}	Standard uncertainty related to a maximum between-unit inhomogeneity that could be hidden by method repeatability; an additional index "rel" is added when appropriate

u_{bb}	Standard uncertainty related to a possible between-unit inhomogeneity; an additional index "rel" is added when appropriate
u_c	Combined uncertainty
u_{cal}	Standard uncertainty of a common calibrant
u_{char}	Standard uncertainty of the material characterisation; an additional index "rel" is added when appropriate
u_{CRM}	Combined standard uncertainty of the certified value; an additional index "rel" is added when appropriate
U_{CRM}	Expanded uncertainty of the certified value; an additional index "rel" is added when appropriate
u_{Δ}	Combined standard uncertainty of measurement result and certified value
u_{deg}	Standard uncertainty corresponding with a potential degradation observed in the stability study
u_{lts}	Standard uncertainty of the long-term stability; an additional index "rel" is added when appropriate
u_{sts}	Standard uncertainty of the short-term stability; an additional index "rel" is added when appropriate
u_{ρ}	Standard uncertainty of the effective particle density; an additional index "rel" is added when appropriate
$\overline{X}$	Arithmetic mean
Δ_{meas}	Absolute difference between mean measured value and the certified value
ν_{eff}	Effective degrees of freedom
$\nu_{MSwithin}$	Degrees of freedom of MS_{within}
ρ_{cal}	Effective particle density of a calibrant
ρ_{CRM}	Effective particle density of the CRM

1 Introduction

1.1 Background

According to the ISO definition, nanoparticles are particles with all three external dimensions between approximately 1 nm and 100 nm [5], that may exhibit unique properties due to their size. To implement the related European Commission's Recommendation (2011/696/EU) on the definition of a nanomaterial [6], and to better understand the properties of nanoparticles, reliable size and size distribution measurements are needed. In this respect, fit-for-purpose reference materials including quality control and calibration materials are necessary.

A variety of techniques exists to analyse the size and size distribution of nanoparticles. As particles have rarely a perfectly spherical shape, different size parameters would need to be carefully investigated in order to determine the effective particle size [7]. Instead, most measurement methods describe the size of the particles with an "equivalent" diameter. Due to differences in the measurement principles of the different methods, they do not all produce the same equivalent particle diameters for the same particle(s). Therefore particle size is a method-defined measurand. The certified, indicative and additional material information particle size values of ERM-FD101b are specified in this report as equivalent diameters corresponding to the methods used, and to the type of distribution reported. A summary of the techniques used in this study is given below.

1. **Centrifugal liquid sedimentation (CLS)** methods [8] use a centrifugal force to settle particles from a suspension and thereby fractionate particles of different size and/or density. CLS instruments contain the suspension in a disc or a cuvette.

   (i) A *disc centrifuge* instrument is based on a hollow, optically clear spinning disc that is partly filled with a liquid (e.g., a sucrose solution). Under the influence of the centrifugal force the liquid is held against the outside edge of the chamber forming a liquid ring. If this ring is created by a series of injections of liquid with decreasing density, the liquid at the outside edge of the ring is denser than the liquid near the inside edge. The latter density is chosen to be slightly higher than the density of the sample's dispersing medium. When the density gradient is created and stabilised a small volume of a dilute suspension of particles is injected into the centre of the spinning disc. A laser light or X-ray beam passes through the liquid near the outside edge of the disc and particles passing the beam reduce the light intensity in proportion to their concentration.

   Disc centrifuges are operated in the line-start or in the homogeneous mode and are either equipped with (laser) light [9] or X-ray absorption [10] optical detection systems. Their rotational speed varies from 500 revolutions per minute (rpm) to 24000 rpm. The instruments either measure the attenuation of light (turbidity) or that of X-rays. The measured sedimentation time is converted to an equivalent particle size using Stokes' law of sedimentation and the effective particle density. For instruments with turbidity optics, the obtained size distribution is light extinction-based, and this can be converted to a particle mass-based distribution using Mie theory. The latter can be further converted to a number-based distribution by calculating the volume of the particles. For instruments with X-ray absorption optics the attenuation of the X-ray beam is directly proportional to the mass of the detected particles and the size distribution is particle mass-based.[1]

   (ii) In the *cuvette centrifuge*, particles do not travel through a pre-constructed density gradient but sediment out of their native dispersant in which they are initially

[1] Note: For a population of particles with uniform density, particle mass-based and particle volume-based size distributions are identical.

homogeneously distributed. Generally, two types of cuvette centrifuges can be distinguished depending on their maximum rotational speed. The first group of instruments have a rotational speed up to 4000 rpm and are equipped with turbidity optics [11]. The second group of cuvette centrifuges, which are known as analytical ultracentrifugation (AUC) instruments, can be operated at rotational speeds up to 60000 rpm. Today's commercially available AUC instruments are typically equipped with Rayleigh interference (refractometry) optics. Such detection system determines the distribution of sedimentation coefficients by measuring the difference in refractive index between a test sample and a reference sample [12]. The difference in refractive index directly corresponds to the mass of the detected particles. Hence, the particle size distribution obtained from the initial sedimentation coefficient distribution, using Stokes' law, is particle mass-based.

2. **Dynamic light scattering (DLS)**, also referred to as photon correlation spectroscopy or quasi-elastic light scattering, measures the fluctuation of light intensity that is scattered by a quiescent particle suspension upon irradiation by a beam of coherent and monochromatic (laser) light [13]. The intensity of the scattered light, which fluctuates in time due to the Brownian motion of the particles, is registered by a highly sensitive photodetector such as a photomultiplier tube (PMT) or an avalanche photodiode (APD). These detectors are commonly positioned at an angle of about 90° or at about 180° with respect to the incident light beam. DLS instruments are intrinsically absolute in nature and instrumental response or signal calibration or correction factors are thus not required. DLS instruments can be classified according to the principle of data acquisition and processing.

   (i) The majority of DLS instruments are operating in the time-domain. These instruments measure the scattered light intensity fluctuations and process this via a digital correlator to extract an intensity correlation function.

   For highly monomodal dispersions of solid spherical particles, the correlation function linearly decays with a rate that is largely proportional to the translational diffusion coefficient of the particles, except for some impact of the rotational diffusion component. The decay rate can be determined by fitting the correlation function with a first-order or exponential function. The (apparent) translational diffusion coefficient then yields, via the Stokes-Einstein relationship, the (apparent) hydrodynamic particle size. In reality, also monomodal samples have a degree of polydispersity. As a result, the correlation function results from a distribution of decay constants and describes a multi-exponential behaviour that can only be fitted approximatively using a cumulants generating polynomial power function. This is generally known as the *method of cumulants* [14,15,16]. The first cumulant of the power function, which corresponds to the initial slope of the correlation function, provides the mean translational diffusion coefficient. The Stokes-Einstein equation then relates the mean translational diffusion coefficient with the scattered light intensity-weighted harmonic mean particle size (or the 'z-average' as it is called in certain commercial DLS software). In addition, a dimensionless qualitative estimation of the degree of polydispersity can be obtained from the ratio of the first and second cumulant. The cumulants method is the most robust, simple and widely used method for measuring the average size of nanoparticles in suspension.

   Contrary to the cumulants method, *distribution calculation algorithms* can be used to compute full particle size distributions (PSDs) by deconvoluting the correlation function via algorithms which include a Laplace transformation. The main disadvantage of Laplace transformation is that the process is mathematically ill-posed: a given correlation function can be described by an infinite number of solutions. The existing algorithms try to overcome this difficulty by using criteria to limit the number of possible solutions and to choose the most reasonable one. One such algorithm, called CONTIN, has been developed by Provencher [17,18]. CONTIN is a generalised inverse Laplace transform algorithm that seeks the simplest (most parsimonious) solution for experimental data based on prior statistical knowledge. The algorithm additionally contains a non-negative

least square (NNLS) routine that is often effectively used as stand-alone PSD algorithm [19]. Another algorithm, called Dynals, behaves similar to CONTIN.

Since a single universally-accepted Laplace transformation algorithm does not exist, most manufacturers of DLS instruments have developed their own specific algorithms that are typically grafted on either the CONTIN or NNLS (or a combination of both) algorithm. Most of these algorithms differ from each other in the grade of smoothing of the correlation function. Because of the different approaches in deconvolution, smoothing and calculation of mean values from the discrete size distributions, and due to sensitivity to noise (from small numbers of larger particles), the results of the distribution calculation algorithms tend to be less repeatable and reproducible than results of the cumulants method. Nevertheless, the advantage of producing full size distributions of different weightings (intensity-, volume- and number-based) has led to a very broad and common use of the distribution calculation algorithms.

(ii) The second group of DLS instruments are equipped with spectrum analysers that obtain the frequency spectra by Fourier transforming the scattered intensity fluctuations into a power spectrum. The power spectrum is then converted into a PSD using a distribution calculation algorithm [20].

3. **Transmission electron microscopy (TEM) and scanning electron microscopy (SEM)** are versatile techniques that allow analysing the morphology, crystallographic structure and chemical composition of nanomaterials. An electron microscope uses an electron source to generate a primary electron beam. In a TEM instrument, a parallel electron beam is created and passes through the very thin specimen. The information contained in the electrons that pass through the specimen is used to create an image. The contrast in this image originates from the absorption and scattering of electrons in the specimen, due to the thickness and composition of the material (i.e. mass-thickness contrast), and from the crystal orientation (i.e. diffraction contrast). An SEM instrument scans the surface of a specimen with a focused beam of electrons. An image is created, for example, by detecting the secondary electrons generated from the interactions of the electron beam with the specimen surface at every point during the scan.

   SEM and TEM instruments have in common that they both produce 2D projections of 3D objects like nanoparticles. To image the nanoparticles, they are deposited onto a suitable substrate (e.g., carbon foils or metal grids, mica surfaces or silicon wafers). Based on the difference in contrast between the nanoparticles and the substrate, well-dispersed nanoparticles can be detected in an image analysis process, by applying grey-level threshold limits, and then be quantified e.g. in terms of particle size and particle size distribution.

   The size of the particles in the electron microscopy (EM) images can be quantitatively defined using different size and shape parameters (e.g., minimum and maximum Feret's diameter, Martin's diameter, projected area-equivalent circular diameter) [21,22,23,24]. Automated, semi-automated and manual image analysis can be performed by using designated software.

4. **Particle tracking analysis (PTA)**, also referred to as nanoparticle tracking analysis, dynamic ultramicroscopy, or orthogonal tracking microscopy, combines laser light scattering microscopy with a digital video camera. The camera records the light scattered by the particles that are moving under Brownian motion. The PTA software detects, based on their scattering behaviour, individual particles suspended in a liquid and monitors their trajectories in the suspension. The movement of the particles, expressed as a mean square displacement, is related to their hydrodynamic diameter via a formula derived from the Stokes-Einstein equation.

5. In **small-angle X-ray scattering (SAXS)**, a narrow beam of X-rays is passed through a sample, e.g., a suspension of nanoparticles [25]. The X-rays are scattered at surfaces of increased electron density, such as the surface of the particles, thereby creating elastic

scattering waves (Rayleigh scattering). These scattering waves interfere with one another forming a scattering pattern. Particles produce maximum scattering at an angle which is inversely related to the particle size. This angle, together with the individual unit vectors in the incident and scattered X-ray directions, is the basis for the scattering vector (q). The shape of the scattering curve contains information of particle size and particle shape.

At small scattering vectors the scattered X-ray intensity only depends on the contrast (= difference in electron density of the particle versus dispersing medium), concentration, particle volume and radius of gyration (R_g). The latter is a size parameter that corresponds to the root mean square (quadratic mean) of the distance to the centre of mass weighted by the contrast of electron density and which can be determined by applying the Guinier law [26]. This initial part of the scattering curve can be approximated by a Gaussian function, hence its natural logarithm versus q^2 yields a straight line. The value of the corresponding Guinier radius, R_G, which can be calculated from the slope of the fitted linear curve is a $(\text{volume})^2$-weighted mean of the size of the particles in the suspension. Following this *Guinier approximation*, only an overall mean particle size can be obtained.

With the information in the SAXS scattering curve at larger q-values, it is also possible to obtain a full PSD. This requires assumption of a certain model PSD distribution, the parameters of which must be fitted to make the experimental scattering curve match the theoretical [27]. This *model fitting* method [28] allows computation of number-, volume- and (X-ray scattering) intensity-based PSDs under the assumption of homogeneous particle shape.

1.2 Choice of the material

Given its industrial relevance, and the ability to remain colloidally stable for several years, silica nanoparticles were selected as target particles.

ERM-FD101b was produced from a commercially available sol which consisted of silica nanoparticles suspended in an aqueous solution of electrolytes. In order to allow the users of ERM-FD101b to use the CRM as-received (e.g., for DLS, SAXS and CLS), the original silica sols were strongly diluted with purified water (18.2 MΩ·cm resistivity at 25 °C). This increases the versatility with respect to the preparation of test specimens for microscopy analysis and it allows using values of physical properties (e.g., viscosity, density, refractive index) that are known for water and which are needed to calculate the equivalent diameters for several particle size analysis (PSA) methods.

1.3 Design of the project

The stability and homogeneity of the material was evaluated through PSA using DLS and CLS. The combined knowledge on the material homogeneity and stability obtained from DLS and CLS measurements is sufficiently detailed to also use the resulting homogeneity and stability uncertainty contributions for the certification of the particle size values obtained with other PSA methods. The certified and indicative values were established by an interlaboratory comparison of different laboratories with different measurement methods and techniques.

2 Participants

2.1 Project management and evaluation

European Commission, Joint Research Centre, Directorate F – Health, Consumers and Reference Materials, Geel, BE
(accredited to ISO Guide 34 for production of certified reference materials, BELAC No. 268-RM)

2.2 Processing

European Commission, Joint Research Centre, Directorate F – Health, Consumers and Reference Materials, Geel, BE
(accredited to ISO Guide 34 for production of certified reference materials, BELAC No. 268-RM)

2.3 Homogeneity study

European Commission, Joint Research Centre, Directorate F – Health, Consumers and Reference Materials, Geel, BE
(accredited to ISO Guide 34 for production of certified reference materials, BELAC No. 268-RM; measurements under the scope of ISO/IEC 17025 accreditation BELAC No. 268-TEST)

2.4 Stability study

European Commission, Joint Research Centre, Directorate F – Health, Consumers and Reference Materials, Geel, BE
(accredited to ISO Guide 34 for production of certified reference materials, BELAC No. 268-RM; measurements under the scope of ISO/IEC 17025 accreditation BELAC No. 268-TEST)

2.5 Characterisation

The participants in the interlaboratory comparison study were (list alphabetical order):

Agfa Gevaert NV, Agfa-Labs, Mortsel, BE

Anton Paar GmbH, Graz, AT

AQura GmbH, Marl, DE
(accredited to ISO/IEC 17025, measurements under the scope of DAkkS No. D-PL-14093-01-00)

Beijing Center for Physical and Chemical Analysis (BCPCA), Beijing, CN
(accredited to ISO/IEC 17025, measurements under the scope of CNAS No. L0066)

BAM Federal Institute for Materials Research and Testing, Berlin, DE

Dannalab B. V., Enschede, NL

Delft Solids Solutions B.V., Wateringen, NL

Dr. Lerche KG, Berlin, DE

European Commission, Joint Research Centre, Directorate F – Health, Consumers and Reference Materials, Geel, BE
(accredited to ISO/IEC 17025, measurements under the scope of BELAC No. 268-TEST)

Horiba Instruments Inc., Irvine, US

Horiba Scientific, Longjumeau, FR

Hungarian Academy of Science, Research Centre for Natural Sciences, Biological Nanochemistry Research Group, Institute of Materials and Environmental Chemistry (RCNS HAS), Budapest, HU

Leidos Biomedical Research Inc, Frederick National Laboratory for Cancer Research, Nanotechnology Characterization Laboratory, Frederick, US

LGC Ltd., Teddington, UK

LUM GmbH, Berlin, DE

Malvern Instruments Inc., Westborough, US

Malvern Instruments Ltd., Malvern, UK

Malvern Instruments Ltd., Amesbury, UK

MicroParticles GmbH, Berlin, DE

MVA Scientific Consultants, Duluth, US

Nanolytics, Gesellschaft für Kolloidanalytik mbH, Potsdam,DE

National Center for Nanoscience and Technology (NCNST), CAS Key Lab for Biomedical Effects of Nanomaterials and Nanosafety, Beijing, CN

National Institute of Metrology (NIM), Division of Nano Metrology and Materials Measurement, Beijing, CN

National Institute of Standards and Technology (NIST), Physical Measurement Laboratory, Semiconductor and Dimensional Metrology Division, Gaithersburg, US

National Measurement Institute Australia (NMIA), Nanometrology, West Lindfield, AU

National Physical Laboratory (NPL), Analytical Science Division, Teddington, UK

Physikalisch-Technische Bundesanstalt (PTB), Working Group 7.11 "X-ray Radiometry", Berlin, DE

Physikalisch-Technische Bundesanstalt (PTB), Working Group 4.22 "Quantitative Microscopy", Braunschweig, DE

Sympatec GmbH, Clausthal-Zellerfeld, DE

Technical University (Bergakademie) Freiberg, Institute for Mechanical Process Engineering and Mineral Processing, Laboratory for Particle Characterisation, Freiberg, DE

TNO, Delft, NL

University of Konstanz, Physical Chemistry, Konstanz, DE

University of Konstanz, Physics Department, Konstanz, DE

University of Namur, Namur Nanosafety Centre, Namur, BE

Veterinary and Agrochemical Research Centre (CODA-CERVA), Electron Microscopy Service, Brussels, BE

3 Material processing and process control

3.1 Origin of the starting material and available information

The colloidal silica starting material Klebosol 30R50 was supplied by AZ Electronic Materials France SAS (Trosly-Breuil, FR). Material specifications for the starting material, as provided by the manufacturer, are listed in Table 1.

In studies prior to the certification project, a number of material properties were assessed:

- The nominal SiO_2 (dry) mass fraction was confirmed by in-house measurements (309 g/kg).
- Preliminary TEM analyses were performed by an independent laboratory (MVA Scientific Consultants, Duluth, USA) qualified by the JRC. TEM grids were dipped in the as-received concentration of colloidal silica, and imaged with a Philips CM120 TEM at an acceleration voltage of 100 kV. A typical TEM micrograph is shown in Fig. 1. The particle aspect ratio, defined as the ratio of the major diameter (length) to the minor diameter (width) of a fitted ellipse, is close to 1.0, indicating a near-spherical morphology.

  The TEM micrograph and the resulting particle size distribution (Fig. 1) show two well-separated particle populations: one at 80 nm and a second one of smaller particles around 40 nm. The population of smaller particles accounts for about 30 % of the total number of particles. The certification exercise on ERM-FD101b was focused on the 80 nm particle population.

Table 1: Information on Klebosol 30R50 starting material provided by the manufacturer

Property	**Specifications / Observations**
Batch identification	19019/L1
Appearance	Milky turbid
Nominal particle diameter	80 nm
Nominal SiO_2 concentration	300 g/kg
Specific surface area	40 m^2/g to 60 m^2/g
Free alkalinity as Na_2O	≤ 0.2 g/kg
pH (at 25 °C)	8.5 to 9.5
Suspension density (at 20 °C)	1.2 g/cm^3

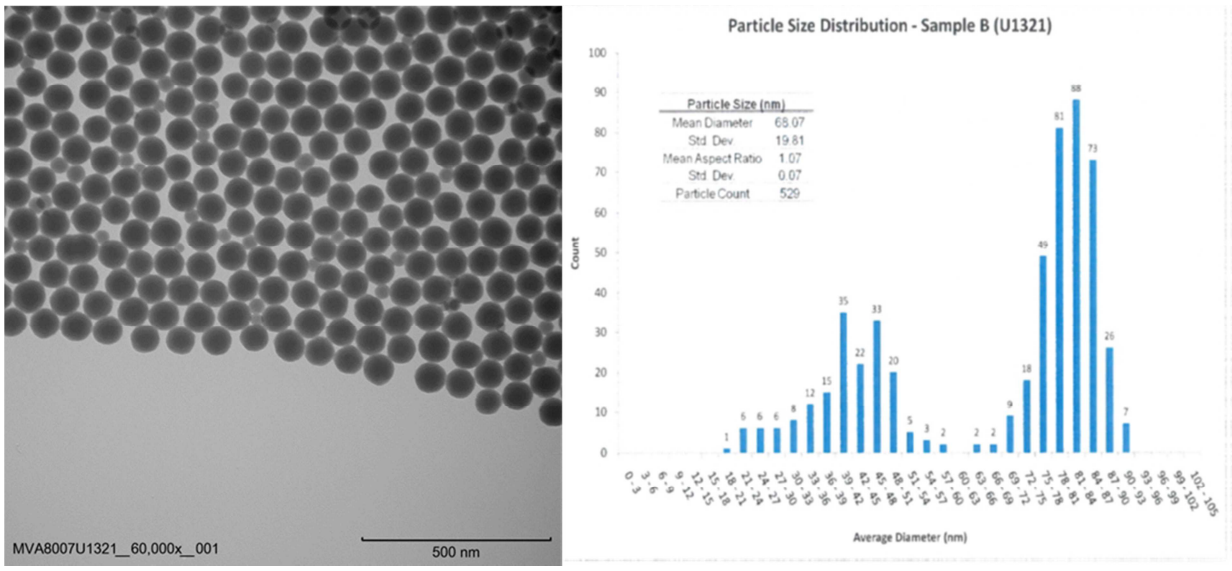

Fig 1 TEM micrograph and number-based area-equivalent PSD of Klebosol 30R50 silica nanoparticles (MVA Scientific Consultants, Duluth, US)

3.2 Processing

The Klebosol 30R50 starting material was diluted to a target nominal SiO_2 mass fraction of 2.5 g/kg, by the addition of purified water (resistivity 18.2 MΩ·cm at 25 °C) produced by an Elix 35 water purification system (Merck Millipore, Molsheim, FR). The diluted Klebosol 30R50 was prepared by addition of 178 g of the initial starting material into 21822 g of purified water. The batch was vigorously hand shaken and rolled several times, flushed with Ar, and left overnight.

On the following day, before preparing the final batch, the suspension was transferred to a new clean bottle. In ensuring that potentially settled contamination was left behind, the lower end of the transfer tube was kept about 5 cm away from the bottom of the bottle. During siphoning, special care was taken to minimise turbulence. Multiple samples were taken from both the originally prepared suspension, the fraction that was left behind in the original bottle and from the final batch. Using DLS, no significant differences were found between the different fractions. Finally, the pH of the final batch was adjusted to pH 9 by adding 0.5 M NaOH. The solution was then flushed with Ar.

Pre-scored 10 mL amber glass ampoules (Nederlandse Ampullenfabriek B.V., Nijmegen, NL) were chosen to provide a rugged and gas tight containment for the colloidal silica samples. Before filling, the ampoules were opened, rinsed with purified water and dried in an oven.

The ampoules were loaded to the Rota ampouling machine R 910 PA (Rota, Wehr, DE). Every ampoule was flushed with Ar gas immediately before filling with about 9 mL of suspension. The suspension in the supply bottle was continuously stirred with a magnetic stirrer throughout the process of filling the ampoules. Immediately after filling, the ampoules were again flushed with Ar and closed. In total 1941 ampoules were produced.

4 Homogeneity

A key requirement for any reference material (RM) produced as a batch of different units is the equivalence between the various units. In this respect, it is relevant whether the variation between units is significant compared to the uncertainty of the certified value. In contrast to that, it is not relevant if this variation between units is significant compared to the analytical variation. Consequently, ISO Guide 34 [1] requires RM producers to quantify the between-unit variation. This aspect is covered in between-unit homogeneity studies.

The within-unit inhomogeneity does not influence the uncertainty of the certified value when the minimum sample intake is respected, but determines the minimum size of an aliquot that is representative for the whole unit. Quantification of within-unit heterogeneity is therefore necessary to determine the minimum sample intake.

4.1 Between-unit homogeneity

The between-unit homogeneity was evaluated to ensure that the certified values of the CRM are valid for all units of the material, within the stated uncertainty.

The number of selected units corresponds to approximately the cubic root of the total number of the produced units. 15 units, selected using a random stratified sampling scheme covering the whole batch, were analysed by DLS and CLS to test the between-unit homogeneity. From each of the 15 units, two independent sub-samples (aliquots) were taken and analysed by means of DLS (cumulants method) following the in-house validated method at a sample temperature of 25 °C. In addition to the DLS measurements, the 15 units were also analysed in triplicate by means of line-start CLS (turbidimetry). The temperature of the CLS gradient was about 29 °C.

The DLS and CLS measurements were performed under repeatability conditions, and in a randomised manner to be able to separate a potential analytical drift from a potential trend in the filling sequence. Regression analyses were performed on the DLS and CLS data to evaluate potential trends in the analytical sequence as well as trends in the filling sequence. Analytical trends were visible and were linearly corrected in some of the CLS and DLS data sets. No trend on the filling was observed.

Quantification of between-unit inhomogeneity was accomplished using analysis of variance (ANOVA), which can separate the between-unit variation (s_{bb}) from the within-unit variation (s_{wb}). The latter is equivalent to the method repeatability if the individual samples are representative for the whole unit. Evaluation by ANOVA requires unit means which follow at least a unimodal distribution and results for each unit that follow unimodal distributions with approximately the same standard deviations. From the obtained histograms and normal probability plots, it was concluded that all data followed a normal and unimodal distribution. Minor deviations from unimodality of the individual values do not significantly affect the estimate of between-unit standard deviations.

Data were checked and scrutinised for single and double outliers by applying the Grubbs' test at a confidence level of 99 %. For both the DLS and CLS results, statistical outliers were neither detected for data grouped according to unit means, nor for data grouped according to individual results.

One has to bear in mind that s_{bb} and s_{wb} are estimates of the true standard deviations and are therefore subject to random fluctuations. Therefore, the mean square between groups ($MS_{between}$) can be smaller than the mean squares within groups (MS_{within}), resulting in negative arguments under the square root used for the estimation of the between-unit variation, whereas the true variation cannot be < 0. In this case, u^*_{bb}, the maximum inhomogeneity that could be hidden by method repeatability, was calculated as described by Linsinger *et al.* [29]. u^*_{bb} is comparable to the limit of detection of an analytical method,

yielding the maximum inhomogeneity that might be undetected by the given study setup. The larger value of s_{bb} or u^*_{bb} was used as uncertainty contribution for homogeneity, u_{bb}.

Method repeatability ($s_{wb,rel}$), between–unit standard deviation ($s_{bb,rel}$) and $u^*_{bb,rel}$ were calculated in accordance to ISO Guide 35 [2]. The results of the evaluation of the between-unit variation are summarised in Table 2.

$$s_{wb,rel} = \frac{\sqrt{MS_{within}}}{\bar{y}} \qquad \textbf{Equation 1}$$

$$s_{bb,rel} = \frac{\sqrt{\frac{MS_{between} - MS_{within}}{n}}}{\bar{y}} \qquad \textbf{Equation 2}$$

$$u^*_{bb,rel} = \frac{\sqrt{\frac{MS_{within}}{n}}\sqrt[4]{\frac{2}{v_{MSwithin}}}}{\bar{y}} \qquad \textbf{Equation 3}$$

MS_{within} mean of squares within a unit from an ANOVA

$MS_{between}$ mean of squares between-unit from an ANOVA

$\bar{y}$ mean of all results of the homogeneity study

n mean number of replicates per unit

$v_{MSwithin}$ degrees of freedom of MS_{within}

Table 2: Results of the homogeneity study for ERM-FD101b

PSA method	$s_{wb,rel}$ [%]	$s_{bb,rel}$ [%]	$u^*_{bb,rel}$ [%]	$u_{bb,rel}$ [%]
DLS [1)]	0.27	0.10	0.12	0.12
CLS [2)]	0.65	0.49	0.19	0.49

[1)] Scattered light intensity-weighted harmonic mean hydrodynamic particle diameter (cumulants method)

[2)] Light extinction-weighted modal Stokes particle diameter (turbidimetry)

The homogeneity study showed no outlying unit means or trends in the filling sequence. Therefore the between-unit standard deviation, $s_{bb,rel}$, can be used as estimate of u_{bb}. As u^*_{bb} sets the limits of the study to detect inhomogeneity, the larger value of $s_{bb,rel}$ and $u^*_{bb,rel}$ is adopted as uncertainty contribution to account for potential inhomogeneity.

4.2 Within-unit homogeneity and minimum sample intake

The within-unit homogeneity is closely correlated to the minimum sample intake. The minimum sample intake is the minimum amount of sample that is representative for the whole unit and thus can be used in an analysis. Sample sizes equal to or above the minimum sample intake guarantee the certified value within its stated uncertainty.

The minimum sample intake was determined from the results of the characterisation study, using the method information supplied by the participants. The smallest sample intake that

still yielded results with acceptable accuracy to be included in the respective studies was taken as minimum sample intake. Using the data from Annex D (Tables D.1 to D.5), the following minimum sample intakes are derived:

- CLS (turbidimetry): 100 µL
- CLS (refractometry): 340 µL
- DLS: 100 µL
- EM: 2.5 µL of an as-received aliquot and analysis of at least 250 discrete particles
- PTA: 1 µL and at least 500 tracks
- SAXS: 20 µL

5 Stability

Time and temperature were regarded as the most relevant influences on stability of the material. The influence of visible radiation was minimised by the choice of the containment (amber glass ampoules) which eliminates most of the incoming light.

Stability testing is necessary to establish conditions for storage (long-term stability) as well as conditions for dispatch to the customers (short-term stability). During transport, especially in summer time, temperatures up to 60 °C may be reached and stability under these conditions must be demonstrated if transport at ambient temperature will be applied.

The stability studies have been carried out using an isochronous design [30]. In that approach, samples are stored for a certain time at different temperature conditions. Systematically, more samples are moved to conditions where further degradation can be assumed to be negligible (reference conditions), effectively "freezing" the degradation status of the material. At the end of the isochronous storage, the samples are analysed simultaneously under repeatability conditions. Analysis of the material (after various exposure times and temperatures) under repeatability conditions greatly improves the sensitivity of the stability tests.

5.1 Short-term stability study

For the short-term stability study, samples were stored at 4 °C and 60 °C for 0, 1, 2 and 4 weeks (at each temperature). The reference temperature was set to 18 °C. For the storage temperatures 4 °C and 60 °C, 4 units were selected per storage time point. For the reference temperature of 18 °C, a total of 4 units were taken. All units were selected from the produced batch using a random stratified sampling scheme. From each unit, two aliquots were measured by DLS (cumulants method, sample temperature of 25 °C) and line-start CLS (disc centrifuge, temperature of the CLS gradient about 29 °C). Each DLS aliquot was measured three times in a consecutive manner. Measurements were equally spread over two consecutive days, the first day the isochronous study at 4 °C, the second day the isochronous study at 60 °C. All measurements were performed in a randomised manner to be able to separate a potential analytical drift from a trend over storage time.

Regression analyses were performed on the DLS and CLS data to evaluate potential trends in the analytical sequence. Analytical drift was visible and was linearly corrected in both CLS and DLS data sets. After having corrected the CLS and DLS results for the analytical drift, data were pooled according to the storage temperatures 4 °C and 60 °C. The new sets of results were then evaluated individually for each temperature. The results were screened for outliers using the single and double Grubbs' tests on 99 % confidence levels. No outlying individual results were found (Table 3). The individual DLS and CLS measurement results are shown in Fig.B1 and Fig.B2 of Annex B.

Furthermore, the data were plotted against storage time, and regression lines of particle diameter *versus* time were calculated. The slopes of the regression lines were then tested for statistical significance (decrease/increase due to shipping conditions). For the DLS and CLS sets of results at 60 °C storage temperature, the slope of the regression lines were found to be significantly different from zero at a confidence level of 95 %. The values of both slopes (0.18 nm/week for DLS and −0.18 nm/week for CLS) indicate statistically significant degradation. However, considering a shipping period of 1 week and the fact that the sample will not be exposed for more than 1 week at 60°C, and noting that the measured slopes are small and contradicting each other, the degradation is considered technically negligible. (During the production of a similar monodisperse, colloidal silica CRM, ERM-FD100, slopes of the regression lines were also found to be statistically significant at a confidence level of

95 %, but technically negligible [31].) Nevertheless, potential degradation over one week according to the measured slopes was included in the uncertainty value.

Table 3: Results of the short-term stability tests

	Number of individual outlying results		Significance of the trend on a 95 % confidence level	
PSA method	**4 °C**	**60 °C**	**4 °C**	**60 °C**
DLS [1)]	None	None	No	Yes
CLS [2)]	None	None	No	Yes

[1)] Scattered light intensity-weighted harmonic mean hydrodynamic particle diameter (cumulants method)

[2)] Light extinction-weighted modal Stokes particle diameter (turbidimetry)

During the production of a similar colloidal silica CRM, ERM-FD304 [32], it was observed that freezing of the suspension significantly affected the particle size distribution measured after thawing. Therefore, ERM-FD101b must be protected against freezing.

Supported by the experimental data and taking into account a maximum dispatch period of one week, it can be concluded that the material can be safely shipped under ambient conditions. Hence, cooled transportation is not required.

5.2 Long-term stability study

For the long-term stability study, samples were stored at 18 °C for 0, 4, 8 and 12 months. The reference temperature was set to 4°C. A total of 4 units per storage time were selected using a random stratified sampling scheme. From each unit, two aliquots were measured by DLS (cumulants method, sample temperature of 25 °C) and line-start CLS (disc centrifuge, temperature of the CLS gradient about 29 °C). Each DLS aliquot was measured three times in a consecutive manner. Due to the high number of units and the relatively long CLS measurement time, measurements could not be performed under strict repeatability conditions. Instead, measurements were equally spread over two different days, with the first replicates analysed on day 1 and the second replicates analysed on day 2. Across each measurement sequence, samples were randomised with respect to storage time and temperature. This approach allowed separating a potential analytical drift from a trend over storage time.

The particle size results obtained by CLS revealed a clear systematic trend throughout each measurement day: the modal value is increasing throughout the analysis sequence. A possible reason was that a fraction of the particles from the previous measurement (e.g. particles from the 40 nm population) had not yet reached the detector before the launch of the next measurement. No analytical drift was observed within the DLS sets of results.

After having corrected the CLS results for the analytical drift, data from both testing days were pooled according to the storage temperature and time. The new sets of results were then screened for outliers using the single and double Grubbs' test. No outlying individual results were found.

The individual DLS and CLS measurement results of the long-term stability measurements are shown in Fig.C1 and Fig.C2 of Annex C. The results of the statistical evaluation of the long-term stability study are summarised in Table 4.

Furthermore, the data were plotted against storage time and linear regression lines of particle diameter *versus* time were calculated. The slope of the regression lines was tested for statistical significance (decrease/increase due to storage conditions). For both CLS and DLS sets of results, the slopes of the regression lines were not significantly different from zero (on a 95 % confidence level) for a storage temperature of 18 °C.

No technically unexplained outliers were observed and none of the trends was statistically significant on a 95 % confidence level for any of the temperatures. The material can therefore be stored at 18 °C.

Table 4: Results of the long-term stability tests

PSA method	Number of individual outlying results	Significance of the trend on a 95 % confidence level
DLS [1)]	None	No
CLS [2)]	None	No

[1)] Scattered light intensity-weighted harmonic mean hydrodynamic particle diameter (cumulants method)

[2)] Light extinction-weighted modal Stokes particle diameter (turbidimetry)

5.3 Estimation of uncertainties

Due to the intrinsic variation of measurement results, no study can rule out degradation of materials completely, even in the absence of statistically significant trends. This means, even under ideal conditions, the outcome of a stability study can only be "degradation is 0 ± x % per given unit of time". It is therefore necessary to quantify the potential degradation that could be hidden by the method repeatability, i.e. to estimate the uncertainty of stability. The corresponding uncertainties of stability during dispatch and storage were estimated as described in [33] for each measurand. For this approach, the uncertainty of the linear regression line with a slope of zero is calculated. The uncertainty contributions $u_{sts,rel}$ and $u_{lts,rel}$ are calculated as the product of the chosen transport time/shelf life and the uncertainty of the regression lines as:

$$u_{sts,rel} = \frac{RSD}{\sqrt{\sum (t_i - \bar{t})^2}} \cdot t_{tt} \qquad \textbf{Equation 4}$$

$$u_{lts,rel} = \frac{RSD}{\sqrt{\sum (t_i - \bar{t})^2}} \cdot t_{sl} \qquad \textbf{Equation 5}$$

RSD relative standard deviation of all results of the stability study

t_i time elapsed at time point *i*

$\bar{t}$ mean of all t_i

t_{tt} chosen transport time (1 week at 60 ºC)

t_{sl} chosen shelf life (24 months at 18 ºC)

For the short-term stability studies, an uncertainty component, u_{deg}, corresponding with the observed statistically significant degradation trends, needs to be combined with the above uncertainties. This contribution is calculated as:

$$u_{\mathrm{deg}} = \frac{b \cdot t_{sl}}{\sqrt{3}}$$ **Equation 6**

b slope of the regression line of the stability data

The following uncertainties were estimated:

- u_{sts}, the uncertainty of degradation during dispatch. This was estimated from the 60 °C studies. The uncertainty describes the possible change during a dispatch at 60 °C lasting for one week, which can be considered to be a realistic transport time.
- u_{lts}, the stability during storage. This uncertainty contribution was estimated from the 18 °C study. The uncertainty contribution describes the possible degradation during 48 months storage at 18 °C.

The results of these evaluations are summarised in Table 5.

Table 5: Uncertainties of stability during dispatch and storage. $u_{\mathrm{sts,rel}}$ was calculated for a temperature of 60 °C and a period of one week; $u_{\mathrm{lts,rel}}$ was calculated for a storage temperature of 18 °C and a period of four years.

PSA method	$\boldsymbol{u_{\mathrm{sts,rel}}}$ **[%]**	$\boldsymbol{u_{\mathrm{lts,rel}}}$ **[%]**
DLS [1)]	0.12	0.98
CLS [2)]	0.14	1.10

[1)] Scattered light intensity-weighted harmonic mean hydrodynamic particle diameter (cumulants method)

[2)] Light extinction-weighted modal Stokes particle diameter (turbidimetry)

After the certification campaign, the released CRM will be subjected to the JRC's regular stability monitoring programme to control and evidence its further stability.

6 Characterisation

The material characterisation is the process of determining the property values of a reference material. This process was based on a series of interlaboratory comparisons (ILCs) of expert laboratories. For each of the method-defined equivalent particle diameters an ILC was set up between laboratories that applied their measurement procedures, but with respect for the standardised elements of the method-defined measurand. Crucial in this characterisation approach is that the measurements must be performed under intermediate precision (on different days) and reproducibility conditions and that the results from different laboratories are independent. This approach aims at randomisation of laboratory bias, which reduces the combined uncertainty.

6.1 Selection of participants

36 laboratories were selected based on criteria that comprised both technical competence and quality management aspects. Each participant was required to operate a quality system and to deliver documented evidence of its laboratory proficiency in the field of size analysis of nanoparticles. Having a formal accreditation was not mandatory, but meeting the requirements of ISO/IEC 17025 [3] was obligatory. Where measurements are covered by the scope of accreditation, the corresponding accreditation number is stated in the list of participants (Section 2).

6.2 Study setup

Each laboratory received three units of the candidate CRM together with a detailed measurement protocol. This protocol included a description of the measurement scheme as well as guidelines for sample handling and relevant measurement method parameters. The involved SAXS, EM, and CLS laboratories were requested to provide six independent results (two replicates per unit). The participating DLS and PTA laboratories were requested to provide nine independent results (three replicates/aliquots per unit) and each aliquot had to be consecutively measured three and five times, respectively. The units for material characterisation were selected using a random stratified sampling scheme and covered the whole batch. At each laboratory, the sample preparations and measurements had to be spread over at least three different days to ensure intermediate precision conditions.

Blinded CRMs were sent as quality control (QC) samples along with the candidate CRMs to allow independent assessment of method trueness. The following quality control samples were used:

- ERM-FD100 (colloidal silica, JRC) for SAXS and EM methods;
- ERM-FD304 (colloidal silica,JRC) for DLS and CLS (turbidimetry) methods;
- Nanosphere Size Standard 3080A (polystyrene latex, Thermo Scientific) for PTA;
- Nanosphere Size Standard 3100A (polystyrene latex, Thermo Scientific) for CLS (refractometry).

The results of the QC samples were used to support the evaluation of the characterisation results, i.e. to ensure reliability of the results obtained on the candidate CRM.

Laboratories were also requested to give realistic estimations of the expanded uncertainties of the mean value of the replicate results. No approach for the estimation was prescribed, i.e. top-down and bottom-up or combinations of both were regarded as equally valid uncertainty estimation procedures.

6.3 Methods used

6.3.1 Centrifugal liquid sedimentation

ERM-FD101b was characterised by means of CLS with different detection systems (i.e. turbidimetry and refractometry) and geometry (i.e. disc and cuvette type). Instruments were operated either in the line-start mode or in the so-called homogeneous mode. All laboratories analysed ERM-FD101b as-received and applied the general guidelines as stipulated in documentary standards ISO 13318-1 [8] and ISO 13318-2 [9]. These documentary standards include both the line-start and homogeneous CLS methods. Most instruments (in particular the disc-based instruments) do not permit imposing a particular sample temperature. Therefore, the measurement protocol did not specify the measurement temperature. Instead, laboratories were requested to report the sample temperature, as measured during the test, or immediately after the end of the test.

The effective particle density of the test material (ERM-FD101b) is needed to calculate the measured sedimentation times to Stokes diameters. During previous studies, the effective density of the silica nanoparticles of the starting material Klebosol 30R50 was determined *in situ* by means of an isopycnic sedimentation approach. The resulting effective particle density was found to be 2.03 g/cm^3 ± 0.06 g/cm^3 [34]. Based on these isopycnic sedimentation tests on similar silica sols and combining this with other "multiple-velocity" sedimentation approaches, the density of the ERM-FD101b silica nanoparticles is estimated to be 2.0 g/cm^3 with an expanded uncertainty of 0.1 g/cm^3 (rectangular probability distribution). This density value is considered SI-traceable because:

- it is determined by combining results from multiple, independent measurement methods;

- the uncertainty of the results of the individual measurement methods mainly depends on the gravimetric preparation of suspensions, which is done using SI-traceably calibrated balances. (Other parameters in the measurement equations are the sedimentation time and, indirectly, the measurement temperature, via the viscosity values of the suspensions.)

An overview of the instrument specifications and measurement conditions is given in Table D.1 of Annex D. The laboratory codes (e.g., L2) are random numbers and do not correspond to the order of laboratories listed in Section 2. The information in this annex is presented as reported by the ILC participants.

6.3.2 Dynamic light scattering

The characterisation of ERM-FD101b by DLS was performed in terms of the scattered light intensity-weighted mean size of the particle size distribution.

Laboratories were asked to perform sample handling, preparation and measurements according to a protocol that followed the documentary standards ISO 13321 [15] and ISO 22412 [16] where possible and that provided additional guidelines where necessary. Measurements on the monomodal colloidal silica QC sample (ERM-FD304) had to be performed using the cumulants method. All measurements were performed on samples in the as-received state. The measurement protocol recommended the use of optical-quality glass (e.g., quartz) cuvettes, but disposable plastic cuvettes were acceptable too. Furthermore, the protocol required measurements to be performed at 25 °C ± 0.3 °C, an equilibration time of 120 s, a viscosity (at 25 °C） of the dispersing medium of 0.8872 mPa·s and a refractive index (at 25 °C) of the dispersing medium of 1.330. From each ampoule, three aliquots had to be taken and each aliquot had to be measured at least three times under repeatability conditions.

For the ERM-FD101b samples, the majority of the laboratories reported both harmonic mean values according to the *cumulants method*, as well as mean values obtained with one of several different (NNLS, CONTIN) *distribution calculation algorithms*. The use of PSD data evaluation algorithms is not covered by the documentary standards ISO 13321 [15] and ISO

22412 [16] valid at the time of the characterisation exercise. The instrument manufacturers follow different approaches to deconvolute the raw data, and to calculate the reported mean values from the discrete (binned) size distributions. It proved difficult to group the datasets obtained with distribution calculation algorithms according to the kind of reported average value (e.g., arithmetic mean, harmonic mean, geometric mean, modal (peak) value) [35]. However, it was noted that the main peak of the ERM-FD101b PSD is sufficiently narrow and symmetric to limit the theoretical differences between the peak averaging approaches used. Therefore, it was decided to group all results obtained with distribution calculation algorithms and to assign one particle size value, representative for the group of commonly used DLS distribution calculation algorithms. This has consequences for the estimation of the uncertainty (see 6.4.2).

An overview of the instrument specifications and measurement conditions is given in Table D.2 of Annex D. The laboratory code consists of a number assigned to each laboratory (e.g., L2) and abbreviation of the distribution calculation algorithm used (e.g., NNLS, CONTIN).

6.3.3 Electron microscopy

SEMs and TEMs were used to characterise ERM-FD101b in terms of area-equivalent circle diameters. It was asked in the technical specifications to count and measure only particles with an equivalent diameter larger than 60 nm. For the obtained number-based PSDs, the modal and median values were determined. To minimise the risk of contamination during the preparation of EM test specimens, participants were recommended to prepare the test specimens in a clean room or in a low contamination environment. The laboratories were asked to analyse the acquired micrographs according to documentary standard ISO 13322-1 [21]. For each prepared test specimen, at least 1000 discrete (i.e. non-touching) particles had to be measured. During the course of the study this requirement was relaxed: it was allowed to also count touching particles, if they were clearly non-overlapping.

An overview of the instrument specifications and measurement conditions is given in Table D.3 of Annex D. The laboratory code consists of a random number assigned to each laboratory (e.g., L2) and abbreviation of the type of EM instrument used (e.g., SEM, TEM).

6.3.4 Particle tracking analysis

The intensity of the light scattered by the particles in undiluted ERM-FD101b in a PTA instrument is too high and as a result individual particles cannot easily be resolved. As a rule of thumb, PTA test samples should contain between 10^7 and 10^9 particles/mL. Therefore, laboratories were asked to dilute the as-received material using purified water (resistivity of 18.2 MΩ.cm at 25°C and additionally filtered through a membrane with nominal pore size of 0.1 μm) depending on the optical specifications of their instruments. To allow determination of the particle concentration, sample loading (and dilution) had to be performed using accurately calibrated micropipettes and/or syringes. Additional measurement conditions that were fixed in the test protocol were: measurement temperature (25 °C ± 0.5 °C), equilibration time between measurements (30 s), viscosity (0.8872 mPa.s at 25 °C) and refractive index of the dispersion liquid (1.330 at 25 °C). The mode, mean and median values of the number-based PSDs had to be reported, as well as the particle concentration.

An overview of the instrument specifications and measurement conditions is given in Table D.4 of Annex D.

6.3.5 Small-angle X-ray scattering

ERM-FD101b was also characterised using SAXS. Measurements were performed on the as-received material. The experimental scattering curves were corrected for background noise. The data were analysed both using the Guinier approximation and the 'model fitting' approach.

In the Guinier approximation, the initial parts (at low *q*-ranges) of the scattering curves were approached with linear regression fits from which the (volume)^2-weighted Guinier radii (R_G) were deduced. These results were then converted into the mean equivalent spherical diameter (*D*) following Equation 7.

$$D = 2\sqrt{\frac{5}{3}}R_G \qquad \textbf{Equation 7}$$

In addition, PSDs were determined by applying the 'model fitting' approach to a broader part of the scattering curve [28].

The laboratories were asked to perform the measurements at a temperature in the range of 20 °C to 30 °C, preferably at 25 °C.

An overview of the instrument specifications, measurement conditions and chosen models is given in Table D.5 of Annex D.

6.4 Evaluation of results

The characterisation campaign resulted in a total of 55 independent datasets. Table 6 summarises the measurands reported for each of the techniques and methods.

Table 6: Measurands and number of independent datasets per technique

Technique (method)	Measurands	Sets
CLS (turbidimetry)	Light extinction-weighted modal Stokes diameter	8
CLS (refractometry)	Mass-based modal Stokes diameter	2
DLS (cumulants method)	Scattered light intensity-weighted harmonic mean hydrodynamic diameter	20
DLS (distribution calculation algorithms)	Scattered light intensity-weighted mean hydrodynamic diameter	14
EM	Number-based area-equivalent diameter (modal, mean)	14
PTA	Number-based hydrodynamic diameter (modal, arithmetic mean, median)	7
SAXS (Guinier approximation)	((Volume)^2)-weighted mean diameter	5
SAXS (model fitting)	Number-, volume-, intensity-weighted modal diameter	5

All individual results of the participants, grouped per technique/method/measurand are displayed in tabular and graphical form in Annex E.

6.4.1 Technical evaluation

The obtained data were first checked for compliance with the requested measurement protocol and for their validity based on technical criteria. The following criteria were considered during the evaluation:

- appropriate validation of the measurement procedure;
- compliance with the provided measurement protocol: sample preparations and measurements performed on three days;

- method performance, i.e. agreement of the measurement results with the assigned value of the QC sample following the procedure described in ERM Application Note 1 [36].

Table 7 shows the datasets rejected as not technically valid based on the above criteria.

Table 7: Datasets that showed non-compliances with the analysis protocol and technical specifications, and action taken

PSA method	Lab-code	Description of problem	Action taken
EM	L9a	Results for QC sample ERM-FD100 did not agree with the certified value within the reported uncertainty	Data not used for evaluation
EM	L9b	Results for QC sample ERM-FD100 did not agree with the certified value within the reported uncertainty	Data not used for evaluation
EM	L29	Modal values for QCM not reported	Data not used for evaluation
DLS	L1	Results for QC sample ERM-FD304 did not agree with the certified value within the reported uncertainty	Data not used for evaluation
DLS	L12	Results for QC sample ERM-FD304 did not agree with the certified value within the reported uncertainty	Data not used for evaluation
DLS	L29	Protocol not followed	Data not used for evaluation
DLS	L32	Results for QC sample ERM-FD304 did not agree with the certified value within the reported uncertainty	Data not used for evaluation

Dynamic light scattering: 19 laboratories were involved in the DLS ILC study. One laboratory submitted 2 data sets. Three laboratories failed on the measurements of the QCM and one laboratory did not follow the measurement protocol. In total 16 data sets were accepted for the cumulants method, and 11 data sets were accepted for the distribution calculation algorithms.

The results of the technical evaluation of the DLS datasets are summarised in Annex E1.

Centrifugal liquid sedimentation: 10 laboratories were involved in the CLS ILC study. Of the 10 laboratories, 4 participated with homogeneous CLS (ultracentrifugation or cuvette) methods. This group is further split into laboratories that used AUC with refractometry (2) and laboratories that performed measurements using benchtop ultracentrifuges equipped with turbidimetry (2). The other six laboratories applied line-start CLS (disc centrifugation) methods with turbidimetry. Because of the different measurands, datasets originating from CLS instruments with turbidimetric detection systems and CLS instruments equipped with refractometric detection (L18 and L28), were evaluated separately.

The results of the technical evaluation of the CLS datasets are summarised in Annex E2.

Electron microscopy: Ten laboratories participated in the ILC study with SEM and TEM methods. A total of 14 datasets were received. Three participants performed measurements using both SEM and TEM, and one participant used an SEM both in scanning mode and in transmission (TSEM) mode. An unpaired two-tailed Students' *t*-test showed no significant difference (significance level 0.05) between the mean values of the two instrument groups.

The results of the technical evaluation of the EM datasets are summarised in Annex E3.

Particle tracking analysis: Seven laboratories participated in the ILC study with PTA. Laboratories also reported the absolute particle number concentration. However, the concentration results varied too much between laboratories. Therefore, the concentration data were considered insufficiently reliable for certification purposes. For PTA, the as-

received material was too concentrated and all laboratories therefore applied high dilution factors (Annex Table D.4). Dilution does affect the ionic strength of the suspension and can thus also have an effect on the colloidal stability, i.e. increased interaction between nanoparticles can lead trigger the formation of agglomerates. While no excessive agglomeration has been reported by the laboratories, the presence of a limited number of small agglomerates explains the slightly, but significantly, higher value for the arithmetic mean particle size compared to the median and modal particle size measurands.

The results of the technical evaluation of the PTA datasets are summarised in Annex E4.

Small-angle X-ray scattering: Five laboratories participated in the SAXS ILC study. Test samples were analysed as-received and the experimental scattering curves were evaluated following both the Guinier approximation and the model fitting approach. An overview of the *q*-ranges used for the Guinier approximation and of the imposed particle morphology models is given in Annex Table D.5-2 and Table D.5-3. The model fitting data were not requested by the JRC, but spontaneously reported by the participants, using one or several of the number-based, volume-based and intensity-based types of PSD. To have a complete set of five PSDs of the same distribution type, several of the reported average values were mathematically transformed at the JRC from one to the missing PSD. This was possible using the straightforward relation between the modal (peak) value of the intensity-, volume- and number-based versions of the near-Gaussian shaped peak in the PSD.

The results of the technical evaluation of the SAXS datasets are summarised Annex E5.

6.4.2 Statistical evaluation

The DLS, CLS (turbidimetry), EM, SAXS and PTA datasets that were accepted on the basis of technical criteria, and used for certification, were statistically evaluated. This evaluation included testing for the normality of dataset means using kurtosis/skewness tests as well as normal probability plots, and testing for outlying means and standard deviations (both at 99 % confidence level) using the Grubbs' and Cochran tests, respectively. Standard deviations within (s_{within}) and between ($s_{between}$) laboratories were calculated using one-way ANOVA. The results of these evaluations are shown in Table 8.

The CLS (refractometry) data sets were not evaluated for their normality and outlying means and standard deviations because only two datasets were available. The main observations are:

CLS: Statistical evaluation of the ERM-FD101b datasets flagged the variances of laboratory L5 and L14 as outliers for the modal Stokes particle diameter by CLS (turbidimetry). In essence, outliers of variance show that repeatability varies between laboratories. The heterogeneity of variances prevents pooling of all individual results, so the evaluation is based on the mean of laboratory means instead. In conclusion, outlying variances are not a reason for exclusion of data.

DLS: The mean value of the mean particle diameter by DLS (cumulants method) of laboratory L6 was detected as an outlier by the Grubbs' test. This mean value is lower than the values reported by the other laboratories. However the difference between the mean value of laboratory L6 and the others is covered by the measurement uncertainties. As there is no clear technical evidence that the results of laboratory L6 significantly deviate from the other results, the data is retained.

SAXS: The variances of laboratories L25 and L35 were determined as outliers for the mean particle diameter by SAXS (Guinier approximation). For the model fitting approach, all laboratories have an outlying variance compared to the very low variance of L22 (synchrotron radiation). As mentioned before, outlying variances are not a reason for exclusion of data.

DLS and PTA: For DLS and PTA methods, the statistical evaluations by Cochran test were out of range, pointing to the difference of standard deviations between the laboratories.

However, as explained before, outlying variances are not a sufficient reason for data exclusion.

Table 8 Statistical evaluation of the technically accepted datasets for ERM-FD101b (*p* = number of technically valid datasets).

PSA method	*p*	Outliers		Normally distributed	Statistical parameters			
		Means	Varian-ces		Mean [nm]	*s* [nm]	$s_{between}$ [nm]	s_{within} [nm]
CLS [1)]	8	None	L5,L14	Yes	86.7	3.6	3.6	0.6
DLS [2)] (cumulants)	16	L6	L5, L24	Yes (acc. skewness test) / No (acc. kurtosis test), due to 1 outlier	89.5	1.9	1.9	0.7
DLS [3)] (distribution calculation algorithms)	11	None	L3b	Yes	93.1	2.1	2.1	0.8
EM [4)] (modal)	11	None	None	Yes	83.7	2.4	2.3	1.3
EM [5)] (median)	11	None	None	Yes	83.5	2.2	2.1	1.2
PTA [6)] (modal)	7	None	None	Yes	81.8	3.8	3.7	1.2
PTA [7)] (median)	7	None	None	Yes	82.2	4.0	4.0	1.2
PTA [8)] (arithmetic mean)	7	None	L20	Yes	86.5	4.3	4.3	1.2
SAXS [9)] (Guinier)	5	None	L25, L35	Yes	86.7	3.6	3.5	1.6
SAXS [10)] (model fit, number)	5	None	L21, L25, L26, L35	Yes	80.9	0.5	0.5	0.7
SAXS [11)] (model fit, volume)	5	None	L21, L25, L26, L35	Yes	81.7	0.6	0.5	0.6
SAXS [12)] (model fit, intensity)	5	None	L25, L35	Yes	82.5	0.8	0.8	0.3

[1)] light extinction-weighted modal Stokes diameter (turbidimetry);
[2)] scattered light intensity-weighted harmonic mean hydrodynamic particle diameter (cumulants method);
[3)] scattered light intensity-weighted mean hydrodynamic particle diameter (distribution calculation algorithms);
[4)] number-weighted modal area-equivalent particle diameter;
[5)] number-weighted median area-equivalent particle diameter;
[6)] number-weighted modal hydrodynamic particle diameter;
[7)] same as [6)] but median;
[8)] same as [6)] but arithmetic mean;
[9)] $((volume)^2)$-weighted mean particle diameter (Guinier approximation);
[10)] number-weighted modal particle diameter (model fitting approach);
[11)] same as [10)] but volume-weighted; [12)] same as [10)] but scattered-X-ray intensity-weighted.

The uncertainty related to the characterisation (u_{char}) was then estimated as the standard error of the means, i.e. $s/\sqrt{p}$ with *s* and *p* taken from Table 8. One exception was made for the values obtained with DLS distribution calculation algorithms. As explained in section 6.3.2, it is not straightforward to link the particle size results obtained with different distribution calculation algorithms to a particular type of mean particle size. Therefore, rather than calculating u_{char} as the standard error of the 11 measured values, it was decided to consider the range of reported values as a rectangular distribution (range = 6.0 nm), with the

midpoint of the interval being the expected value and the corresponding standard uncertainty equal to (range)/(2·√3). This approach provides the most neutral assessment of the reported data and assigns the same weight to each instrument and software represented in the set of accepted data.

An overview of the estimated uncertainties for characterisation is shown in Table 9.

Table 9: Uncertainty of characterisation for ERM-FD101b

PSA method	*p*	Mean [nm]	*s* [nm]	u_{char} [nm]
CLS [1)]	8	86.7	3.6	1.3
DLS [2)] (cumulants)	16	89.5	1.9	0.5
DLS [3)] (distribution calculation algorithms)	11	92.5 [13)]	6.0 [13)]	1.7
EM [4)] (modal)	11	83.7	2.4	0.8
EM [5)] (median)	11	83.5	2.2	0.7
PTA [6)] (modal)	7	81.8	3.8	1.4
PTA [7)] (median)	7	82.2	4.0	1.7
PTA [8)] (arithmetic mean)	7	86.5	4.3	1.6
SAXS [9)] (Guinier)	5	86.7	3.6	1.6
SAXS [10)] (model fit, number)	5	80.9	0.5	0.2
SAXS [11)] (model fit, volume)	5	81.7	0.6	0.3
SAXS [12)] (model fit, intensity)	5	82.5	0.8	0.4

[1)] light extinction-weighted modal Stokes diameter (with turbidimetry);
[2)] scattered light intensity-weighted harmonic mean hydrodynamic particle diameter (cumulants method);
[3)] scattered light intensity-weighted mean hydrodynamic particle diameter (distribution calculation algorithms);
[4)] number-weighted modal area-equivalent particle diameter;
[5)] as in [4)] but median;
[6)] number-weighted modal hydrodynamic equivalent particle diameter;
[7)] as in [6)] but median;
[8)] as in [6)] but arithmetic mean;
[9)] ((volume)^2)-weighted mean particle diameter (Guinier approximation);
[10)] number-weighted modal particle diameter (model fitting approach);
[11)] as in [10)] but volume-weighted; [12)] As in [10)] but scattered-X-ray intensity-weighted;
[12)] not 'mean' and 's' but 'midpoint of interval' and 'range' (maximum value – minimum value).

7 Value Assignment

Certified, indicative and information values were assigned for ERM-FD101b.

Certified values are values that fulfil the highest standards of accuracy. Procedures at the JRC, Directorate F require generally pooling of not less than six datasets to assign certified values. (An exception was made for the highly reproducible SAXS data analysed with the model fitting approach (u_{char} < 0.5 %). The low number of accepted data sets (5) is accounted for by applying the Welch-Satterthwaite equation when expanding the corresponding combined measurement uncertainty.) Full uncertainty budgets in accordance with the 'Guide to the Expression of Uncertainty in Measurement' [4] were established.

Indicative values are values where either the uncertainty is deemed too large or where too few independent datasets were available to allow certification. Uncertainties are evaluated according to the same rules as for certified values.

Additional material information refers to values that were obtained in the course of the study. For example, results reported from only one or two laboratories or in cases where individual measurement uncertainty is high, would fall under this category.

7.1 Certified values and their uncertainties

The unweighted mean of the means of the accepted CLS (turbidimetry), DLS, PTA, SAXS (model fitting approach) and EM datasets, as shown in Table 8 were assigned as certified values for the different measurands.

The assigned uncertainties consist of uncertainties related to characterisation, u_{char} (Section 6), potential between-unit inhomogeneity, u_{bb} (Section 4), potential degradation during transport (u_{sts}) and long-term storage, u_{lts} (Section 5).

For the CLS method, an additional uncertainty stems from the density of the ERM-FD101b particles. Furthermore, as the majority (6 out of 8) CLS datasets were obtained with a disc centrifuge requiring calibration, and since, with the exception of one, all CLS datasets obtained with calibration used PVC calibrants that were supplied by CPS Instruments, Inc., an uncertainty contribution corresponding with the accuracy of the assigned size and density values of these calibrants is also added to the overall uncertainty budget:

- The uncertainty related to the effective particle density ($u_{\rho,CRM}$) was included, following the approach in a previous certification exercise [37]. As described in section 6.3.1, the ERM-FD101b particle density is ρ = 2.0 g/cm^3 ± 0.1 g/cm^3. Assuming a rectangular probability distribution ($\nu_\rho = \infty$), u_ρ is 0.058 g/cm^3. To calculate from this value the corresponding uncertainty of the Stokes diameter requires calculation of the partial derivative of the Stokes' law to the particle density. For a typical set of sedimentation times, Stokes diameters and densities of PVC calibrants and ERM-FD101b, the conversion factor is 33 nm/(g/cm^3).

- The density of the calibrant particles ρ_{cal} = 1.385 g/cm^3 has an expanded uncertainty of 3.5 % [38]. The corresponding standard uncertainty is 0.048 g/cm^3. To calculate from this value the corresponding uncertainty of the Stokes diameter, $u_{\rho,cal}$, requires calculation of the partial derivative of the Stokes' law to the calibrant particle density. For a typical set of sedimentation times, Stokes diameters and densities of PVC calibrants and ERM-FD101b, the conversion factor is 85 nm/(g/cm^3).

- The uncertainty of the Stokes diameters assigned to the calibrants is 5 % [38]. For an average calibrant size of 250 nm, the corresponding standard uncertainty is 6.3 nm. To calculate from this value the corresponding uncertainty of the Stokes diameter, $u_{d,cal}$, requires calculation of the partial derivative of the Stokes' law to the calibrant particle size. For a typical set of sedimentation times, Stokes diameters and densities of PVC calibrants and ERM-FD101b, the conversion factor is 0.25 nm/nm.

The different contributions were combined to estimate the expanded, relative uncertainty of the certified value (U_{CRM}) with a coverage factor k as:

$$U_{CRM,rel} = k \cdot \sqrt{u^2_{char,rel} + u^2_{bb,rel} + u^2_{sts,rel} + u^2_{lts,rel} + u^2_{\rho,CRM,rel} + u^2_{\rho,cal,rel} + u^2_{D,cal,rel}} \qquad \textbf{Equation 8}$$

- u_{char} was estimated as described in Section 6
- u_{bb} was estimated as described in Section 4
- u_{sts} was estimated as described in section 5
- u_{lts} was estimated as described in Section 5
- $u_{\rho,CRM}$ was estimated as described in Section 7.1 (only for CLS)
- $u_{\rho,cal}$ was estimated as described in Section 7.1 (only for CLS)
- $u_{D,cal}$ was estimated as described in Section 7.1 (only for CLS)

Because of the sufficient numbers of the degrees of freedom of the different uncertainty contributions, a coverage factor k = 2 was applied, to obtain the expanded uncertainties.

The certified values and their uncertainties are summarised in Table 10.

Table 10: Certified values and their uncertainties[12)] for ERM-FD101b

PSA method	Certified value [nm]	u_{char} [%]	u_{bb} [%]	u_{sts} [%]	u_{lts} [%]	$u_{\rho,CRM}$ [%]	$u_{\rho,cal}$ [%]	$u_{D,cal}$ [%]	$U_{CRM,rel}$ [%]	U_{CRM} [nm]
CLS [1)]	87	1.46	0.49	0.14	1.10	2.20	2.38	1.80	8.4	8
DLS [2)] (cumulants)	89.5	0.54	0.12	0.12	0.98	n.a.	n.a.	n.a.	2.5	2.3
DLS [3)] (distribution calculation algorithms)	93	1.86	0.12	0.12	0.98	n.a	n.a	n.a	4.3	4
EM [4)] (modal)	83.7	0.85	0.12	0.12	0.98	n.a.	n.a.	n.a.	2.7	2.2
EM [5)] (median)	83.5	0.80	0.12	0.12	0.98	n.a.	n.a.	n.a.	2.6	2.2
PTA [6)] (modal)	82	1.74	0.12	0.12	0.98	n.a.	n.a.	n.a.	4.0	4
PTA [7)] (median)	82	2.01	0.12	0.12	0.98	n.a.	n.a.	n.a.	4.5	4
PTA [8)] (arithmetic mean)	87	1.88	0.12	0.12	0.98	n.a.	n.a.	n.a.	4.3	4
SAXS [9)] (model fit, number)	80.9	0.30	0.12	0.12	0.98	n.a.	n.a.	n.a.	2.1	1.7
SAXS [10)] (model fit, volume)	81.7	0.32	0.12	0.12	0.98	n.a.	n.a.	n.a.	2.1	1.8
SAXS [11)] (model fit, intensity)	82.5	0.43	0.12	0.12	0.98	n.a.	n.a.	n.a.	2.2	1.8

[1)] light extinction-weighted modal Stokes diameter (turbidimetry);

[2)] scattered light intensity-weighted harmonic mean hydrodynamic particle diameter (cumulants method);

[3)] scattered light intensity-weighted arithmetic mean hydrodynamic particle diameter;

[4)] number-weighted modal area-equivalent particle diameter;

[5)] number-weighted median area-equivalent particle diameter;

[6)] number-weighted modal hydrodynamic particle diameter;

[7)] same as [6)] but median;

[8)] same as [6)] but arithmetic mean;

[9)] number-weighted modal particle diameter (model fitting approach);

[10)] as in [9)] but volume-weighted; [11)] as in [9)] but scattered-X-ray intensity-weighted;

[11)] expanded (k = *2*) and rounded uncertainty

In the given study, homogeneity and stability experiments were conducted under repeatability conditions by means of DLS and CLS (turbidimetry) methods. While CLS has a superior resolution for detecting particles of different size and density, DLS is more sensitive in detecting agglomerates. For that reason, the combined knowledge on the material homogeneity and stability obtained from DLS measurements is considered sufficiently detailed to also use the resulting homogeneity and stability uncertainty contributions (i.e. u_{bb}, u_{sts} and u_{lts}) as realistic contributions in the calculations for the uncertainties of the SAXS, EM and PTA measurands.

7.2 Indicative values and their uncertainties

Indicative values were assigned to the ((volume)^2)-weighted mean particle diameter obtained by SAXS measurements (Guinier approximation). Technically valid datasets were received from five different laboratories. The size data were obtained in a range of scattering vectors q varying between 0.025 nm^{-1} and 0.070 nm^{-1}. For the size of the ERM-FD101b particles, this q-range is near the edge of validity of the Guinier approximation. Therefore the resulting value was not certified but is provided as an indicative value instead.

The uncertainty budget (Table 11) was set up in a similar way as for the certified values. The individual standard uncertainties were taken from the DLS homogeneity and stability studies. In contrast to the certified values, where a fixed coverage factor of $k = 2$ was used to expand the uncertainty, the combined uncertainty of the indicative value was multiplied with a t-factor extracted from the t-distribution table following calculation of the effective degrees of freedom according to the Welch-Satterthwaite equation [4].

$$\nu_{\text{eff}} = \frac{u_c^4(y)}{\sum_{i=1}^{N} \frac{u_i^4(y)}{\nu_i}} \qquad \text{(Eq. 8)}$$

ν_{eff}	effective number of degrees of freedom
u_c	combined uncertainty
u_i	individual standard measurement uncertainties
ν_i	degrees of freedom corresponding to u_i

This approach is required if the standard uncertainties are estimated from evaluations with an insufficient number of degrees of freedom to obtain the required 95 % confidence level when using a $k = 2$ coverage factor. For the (volume)^2-weighted mean particle diameter (SAXS, Guinier approximation) the main uncertainty contribution is $u_{char,rel}$. Since at the same time this uncertainty contribution has the smallest number of degrees of freedom, ν_{eff} could be estimated by $\nu_{char} = 4$. Hence the t-factor is 2.78 (for a 95% confidence level).

Table 11: Indicative value and uncertainty for ERM-FD101b

PSA method	**Indicative value [nm]**	$u_{char,rel}$ **[%]**	$u_{bb,rel}$ **[%]**	$u_{sts,rel}$ **[%]**	$u_{lts,rel}$ **[%]**	$U_{CRM,rel}$ **[%]**	U_{CRM} **[nm]**
SAXS[1)]	87	1.86	0.12	0.12	0.98	5.9	6 [2)]

[1)] ((Volume)^2)-weighted mean particle diameter (Guinier approximation) valid in a temperature range of [25 ± 5] °C

[2)] with coverage factor $t = 2.78$ (for a $\nu_{\text{eff}} = 4$, calculated from Equation 9)

7.3 Additional material information

A number of particle properties were also assessed but only at one or two laboratories. The evaluated results are listed as additional material information values. These values must be regarded as informative only on the general properties of the material and cannot be, in any case, used as certified or indicative value.

7.3.1 Centrifugal liquid sedimentation (refractometry)

For the mass-weighted modal Stokes diameter obtained by CLS (refractometry) two well-matching sets of data were received. The average value of both laboratories is provided as an information value.

Table 12: Additional material information value obtained by CLS (refractometry)

Particle sizing method	Information value [nm]
CLS [1)]	84

[1)] Mass-weighted modal Stokes particle diameter (refractometry) at 25 °C ± 1 °C, using an effective particle density of 2.0 g/cm^3

7.3.2 Field flow fractionation

The JRC, Directorate F analysed ERM-FD101b using an asymmetrical flow field-flow fractionation (AF4) instrument which was coupled to a multi-angle light scattering (MALS) detector. Instrumental details are listed in Table D.6 of Annex D. This set-up was used to measure particle size in two different ways.

1) At any given elution time, the particles entering the MALS induce a scattering intensity that depends on the scattering angle. The MALS detectors, placed at 21 different angles, capture the angular dependence of the scattering intensity. This dependency was used to calculate radii of gyration, which were transformed into hydrodynamic radii or diameters. A fractogram representative for ERM-FD101b is given in Fig. 2.

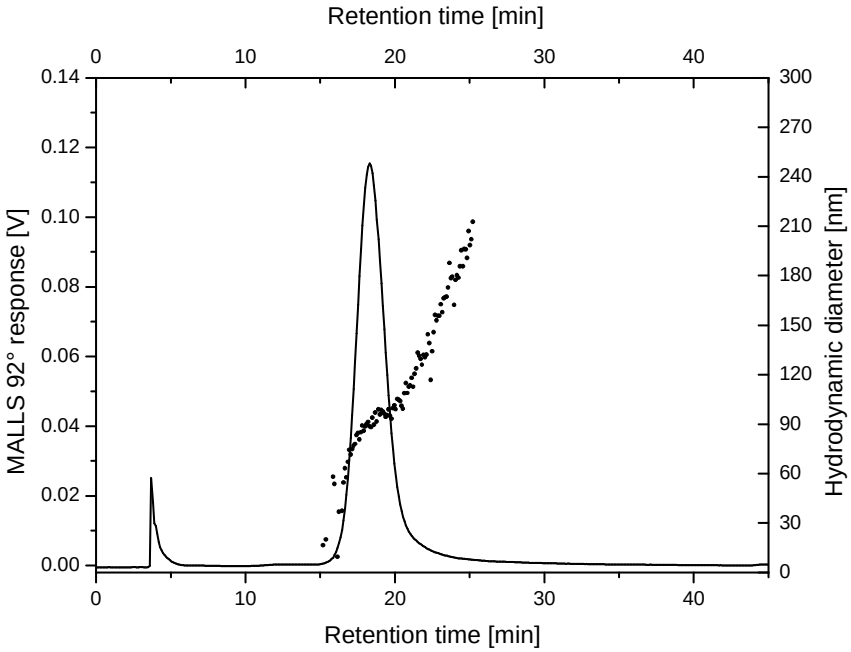

Fig 2 Light scattering intensity fractogram (solid line) obtained using AF4-MALS (92º signal). The dotted curve indicates the hydrodynamic diameter of the particles eluting after the indicated retention time.

2) Calibration curves (retention time versus particle size) were established using different polystyrene latex (PSL) size standards with narrow size distribution and using the maxima of the analytical peaks as given by the 92º angle signal of the MALS detector. Both a linear as well as a double-logarithmic calibration curve were established, the latter providing a better correlation coefficient (R^2 = 0.995) than the former (R^2 = 0.989). The corresponding results (averages of 12 replicates) are given in Table 13.

Table 13: Additional material information values for ERM-FD101b obtained by AF4

Particle sizing method	Information value [nm]
AF4-MALS (92°) [1)]	86
AF4-MALS (92°) [2)]	83

[1)] Scattered light intensity-weighted modal hydrodynamic diameter at 35 °C ± 1 °C, calculated via a calibration curve using a linear scale

[2)] Same as [1)] but calculated via calibration curve using a double logarithmic scale

7.3.3 Electrochemical properties

JRC, Directorate F also reported pH, zeta potential and electrolytic conductivity results (Table 14); instrumental details are listed in Table D.7 of Annex D.

Table 14: Additional material information values

Measurement method	Information value
Zeta potential [1)]	-49 mV
pH [2)]	8.7
Electrolytic conductivity [3)]	0.03 mS/cm

[1)] As obtained by electrophoretic light scattering (ELS) at 25 °C ± 1 °C

[2)] As determined by a potentiometric method at 22 °C ± 1 °C

[3)] Determined at 25 °C ± 1 °C using a folded capillary cell (Malvern Zetasizer Nano ZS instrument)

7.3.4 Sub-population of smaller particles

As mentioned in section 3.1 (Origin of the starting material), a sub-population of smaller particles can be seen in the EM micrographs (Fig. 1). Due to the small size of this particles and their lower number, not all the techniques used during the ILC could detect or quantify them. However, some laboratories did report the presence of this population:

- Lab 18 performed Analytical Ultracentrifugation (AUC). Assuming that the 40 nm particles have the same particle density, Lab 18 estimated their mass fraction at 5 %.
- Lab 16 showed that this sub-population is revealed in the volume-weighted PSD obtained with line-start CLS (turbidimetry), but not in the intensity-weighted PSD.
- The technical specifications for the EM tests asked to count and measure only particles above 60 nm. Nevertheless, L13 reported that the sub-population of small particles accounts for around 40 % of the total number of particles. Also Lab 20 performed EM tests and reported the presence of the sub-population with a mode centred around 40 nm. The total number of particles in that mode was 30 % of that observed for the main population centred at 80 nm. In the PSD, both particle populations are baseline separated.
- Lab 25 reported SAXS data showing a sub-population at 30 nm (volume-weighted PSD). Also Lab 26 mentioned a sub-population near 40 nm, but their contribution to the total scattering intensity was too small to enable a reliable determination of their mean size.

8 Metrological traceability and commutability

8.1 Metrological traceability

Identity

The term 'particle size' is not very specific, as there are multiple size parameters for a single particle, especially if it is not of regular shape. Most PSA methods produce an equivalent diameter (or radius). The actual realisation of the term "equivalent" strongly depends on the nature of the measurement principle of each method.

ERM-FD101b has been characterised using multiple PSA methods and the different assigned property values are intrinsically linked to their corresponding operationally-defined measurands. The certified values can be regarded as reliable estimates of the true equivalent particle sizes, and are underpinned by the agreement of the laboratories' results with the assigned values for the CRMs (ERM-FD100 and ERM-FD304) that were used as QC samples.

All certified size values of ERM-FD101b, except the values obtained with electron microscopy, are valid only in a specified temperature range:

- For the DLS, SAXS and PTA methods, the certified values are valid in the range [25 ± 5] °C. JRC performed DLS tests during which sample temperature was systematically varied in this range. The observed trend was statistically significant (0.1 nm/°C) but, due to the restriction of the allowed testing temperature, it is technically insignificant compared to the uncertainty of the apparent hydrodynamic diameter. For the SAXS method, the size values reflect the size of the core silica particles, and are less dependent on changes of the surface layer of the silica particles. This justifies extrapolating the conclusions on temperature effects from the DLS experiments to the SAXS data.

- For the CLS method, the certified value is valid in the range [25 °C, 36°C].

All accepted CLS characterisation data were obtained in the above specified temperature range. Within the specified temperature ranges, there is no significant trend between the reported size values and the reported measurement temperatures.

The combination of restricting the validity of the certified value to a limited temperature range, and the absence of a technically significant trend within the specified range, justifies the absence of a specific temperature uncertainty contribution in the uncertainty budget of the certified values.

Quantity value

Metrological traceability of the assigned particle size values to a higher order accepted reference, ultimately to a practical realisation of the definition of a unit of the International System of Units (SI) such as the metre, requires traceability of all relevant input factors through an unbroken network of calibrations. Properly characterised and fit-for-purpose calibrants are essential links in order to establish the traceability network. Considering the method-defined nature of the different measurands, the traceability network and final references have been specific for each method. A summary of the traceability network for the different methods used in this study is given below. Detailed information regarding the calibrants used by the different laboratories in the study is listed in the tables of Annex D.

Centrifugal liquid sedimentation (turbidimetry):

The measurand of the CLS method, being the light extinction-weighted modal Stokes particle diameter, is defined by the procedures described in documentary standards ISO 13318-1 [8] and 13318-2 [9].

Whereas the cuvette methods do not require calibration for particle size, the sedimentation time scales of the disc centrifuges were all calibrated using particle size standards. With the exception of one laboratory, all laboratories requiring calibration used PVC calibrant beads that were supplied by CPS Instruments, Inc. The certificates of these calibrants suggest that the assigned values are SI-traceable but there is no documentation available to substantiate this claim. Therefore, a series of these PVC standards of different particle size has been checked in-house against each other as well as against colloidal silica and polystyrene materials. The obtained results [38] indicate consistency, in terms of particle size, amongst the different PVC standards. In addition, a few of the CPS calibrants were subject of a collaborative study involving different laboratories [38]. The study showed that the modal particle diameter, as well as the effective particle density, which are assigned to the PVC calibrants are accurate within 5 % and 3.5 % respectively (95 % confidence level). The conclusion is that, when using the PVC calibrants with traceable particle density and size, the particle size results from well-executed disc-CLS measurements are traceable to the SI unit of length. The uncertainties about the PVC calibrants size and density, as well as that of the SI-traceable particle density value of the ERM-FD101b particles, have been included in the uncertainty of the certified value obtained by CLS (turbidimetry), which therefore is also traceable to the SI.

Dynamic light scattering:

The scattered light intensity-weighted mean hydrodynamic particle diameters, as determined by the cumulants method and by the distribution calculation algorithms, are method-defined. Since the DLS method is intrinsically absolute in nature, there is no need for instrument response calibration or for introducing corrective terms. Traceability of the measured diameter values depends on the traceability of the values corresponding with the parameters occurring in the Stokes-Einstein equation:

- Temperature: the sample temperatures have been measured by sensors which had either been accurately calibrated by their manufacturer or which had been verified following alpha testing using Pt100 sensors.
- Detector angle: the angles at which the detectors were fixed had been geometrically determined as they depend on the mechanical design of the DLS systems. The accuracy of the angle is assured by respecting the applied mechanical tolerances.
- Measured decay rate: the traceability of the measured decay rates depends on the accurately known constant resonant frequency of quartz crystal oscillators that are integrated in programmable logic devices such as a field-programmable gate array (FPGA).
- Refractive index and viscosity of the sample/particle: refractive index and viscosity values were obtained from tables in the literature (e.g., CRC Handbook) reporting traceably measured values.
- Laser wavelength: traceability of the wavelength value to the SI was assured by using helium-neon lasers with a nominal wavelength of 633 nm. In the ILC study, 15 out of the 20 DLS instruments were equipped with such a laser. Unstabilised He-Ne lasers of 633 nm are used in most laser interferometers and many instruments used for length measurements. These instruments, including DLS instruments, are very often used at uncertainty levels that are large compared to the possible variation of the He-Ne laser vacuum wavelength. Based on these considerations, the International Committee of Weights and Measures (CIPM) recognised the need for providing documentary evidence regarding the value of the vacuum wavelength and its uncertainty that can be expected in the absence of calibration. During its 96^{th} meeting, the CIPM adopted a wavelength of 632.9908 nm with a relative standard uncertainty of 1.5×10^{-6} [39]. Following thorough evaluation of the Consultative Committee for Length (CCL) of the CIPM, the CCL

recommended including unstabilised red He-Ne lasers, operating on the 633 ($3s_2 \rightarrow 2p_4$) neon transitions, in the new list of standard frequencies, "*Recommended values of standard frequencies for applications including the practical realization of the metre and secondary representations of the second*". This list replaces the *Mise en Pratique* for the definition of the metre.

Because of the calibration or traceable values of these input parameters, the certified value and uncertainty of the hydrodynamic diameters obtained with DLS are traceable to the SI.

Electron microscopy:

The measurands investigated by SEM and TEM were the number-weighted modal and median area-equivalent particle diameters. The magnifications of the instruments were calibrated using different types of standards which were all suitable for calibration of lateral dimensional measurement systems. Some laboratories used in-situ calibrants in the form of PS particle CRMs. Several laboratories used pitch size standards that were calibrated on a metrological atomic force microscope, thereby linking the assigned pitch dimensions to the SI unit metre through the calibrated laser light wavelength of the interferometer. Other laboratories relied on a calibration via the interplanar distance of a Si crystal. Hence, the certified value and uncertainty are traceable to the SI through the SI traceable values of the calibrants used by the different laboratories.

Particle tracking analysis:

The measurands investigated by PTA are the number-weighted-modal, arithmetic mean and median hydrodynamic particle diameters. Traceability of the measured diameter values depends on the traceability of the values corresponding with the parameters occurring in the modified Stokes-Einstein equation:

- Temperature: temperature has a direct impact on the measured hydrodynamic diameters, as it is a parameter in the Stokes-Einstein equation itself, but also because it has an influence on viscosity. Sample temperature therefore is measured by sensors (thermistor) and controlled by an integrated temperature control (a Peltier controlled with a PID feedback loop). Temperature sensors are usually calibrated by their manufacturer. Possible inaccuracies or instabilities of the temperature sensor calibrations are not expected to contribute to the uncertainty of the certified values of the hydrodynamic diameters measured with PTA beyond the values reported in Section 7.
- Viscosity of the sample/particle: viscosity values were obtained from tables in the literature (e.g., CRC Handbook) reporting traceably measured values.
- PTA instruments measure the length of particles' trajectories and as a consequence a calibration of the measured distances is required. The corresponding calibration of the video image pixel size has been performed by the instrument manufacturer, first via measurements on 10 micrometre pitch graticules and later, more indirectly, via PSA tests on certified polystyrene latex particle size standards (ThermoScientific, 3200 series). The certified values of the latter size standards are SI-traceable, as indicated on their certificate and as documented in [40].
- Time: the traceability on time measurement depends on the accurately known constant resonant frequency of quartz crystal oscillators that are integrated in programmable logic devices. The accuracy of time measurements with such devices is sufficient to exclude significant effects on the uncertainty of the hydrodynamic diameters measured with PTA.
- In order to detect deviations from a proper calibration status, most of the participating laboratories verify their instruments with a variety of quality control materials and calibrants (see Table D.4).

Because of the calibration or traceable values of these input parameters, the certified value and uncertainty of the hydrodynamic diameters obtained with PTA are traceable to the SI.

Small-angle X-ray scattering:

The measurands investigated by SAXS are the scattered X-ray intensity-, number- and volume-weighted modal particle diameters. Traceability of the measured diameter values to the SI unit of length directly depends on the traceability of the values corresponding with the parameters occurring in the equation linking scattering vector (q) and measured scattering angle (θ): $q = 4\pi/\lambda \sin\theta$. Several set-ups were used in the laboratories participating in the interlaboratory characterisation study, and different calibration approaches were followed.

- Half of the scattering angle (θ): either directly measured using (i) a calibrated goniometer, or (ii) geometrically calculated from the calibrated detector pixel size and the sample-to-detector distance. For the second approach, the absolute sample-to-detector distance is determined through standard distance measurements. The detector pixel size is derived from the scattering angle(s) of a suitable reference material (e.g., silver behenate).
- X-ray wavelength: traceability of the x-ray wavelength value to the SI unit metre was assured via back-reflection from appropriate monochromators or single crystals (e.g. silicon) with known lattice constant, or through the nominal wavelength of the Cu-Kα characteristic X-radiation.

The variety of calibration approaches used in the interlaboratory study ensures absence of a systematic bias between laboratories and therefore justifies the decision not to add a specific uncertainty component into the overall uncertainty budget.

8.2 Commutability

According to ISO Guide 34 [1], the assessment of commutability for a CRM requires a comparison and establishment of a numerical correlation between the property value assigned to the CRM and to routine test samples using both a "higher-order" reference measurement procedure and one or more "lower-order" routine measurement procedures. If the ratio between the results of the compared measurement procedures is the same as the ratio of the results for routine test samples, then the CRM is said to be commutable.

ERM-FD101b has been characterised by multiple techniques and methods which all target different method-defined measurands and the size measurement results for near-spherical particles are uncorrelated. Therefore, commutability cannot be assessed. It can be mentioned however that the ERM-FD101b colloidal silica is representative for the routine tests samples encountered in daily laboratory practice.

9 Instructions for use

9.1 Safety information

This material should be handled with care. Nanoparticles can have an impact on environment and human health. Any spilling of the suspension should be handled according to the usual laboratory safety precautions.

For further details refer to the safety data sheet.

9.2 Storage conditions

The materials shall be stored at 18 °C ± 5 °C. Ampoules must not be allowed to freeze, as this will irreversibly compromise the integrity of the material.

Please note that the European Commission cannot be held responsible for changes that happen during storage of the material at the customer's premises, especially of opened ampoules.

9.3 Instructions for use and intended use

The intended use of ERM-FD101b is to check the performance of instruments and/or methods that characterise the size distribution of particles in the range around 100 nm that are either suspended in a liquid medium or deposited onto a suitable substrate. The certified values are regarded as reliable estimates of the true values and ERM-FD101b can therefore be used for calibration purposes.

Before opening, the ampoule should be gently inverted several times to ensure the homogeneity of the suspension and to re-suspend any settled particles. Remove any suspension that remains in the upper part (conical tip) of the ampoule by gently flicking the conical part with the forefinger while tilting the ampoule. The ampoule is pre-scored and can be opened by applying moderate pressure with one's thumb to snap off the conical part. The contents of an ampoule should be used the same day as opened and should be gently homogenised before every measurement, without introducing air bubbles.

DLS method: Aliquots of ERM-FD101b shall be measured as-received, i.e. without dilution. The measurement temperature shall be within the range [25 ± 5] °C. The viscosity and refractive index of the dispersing medium (water) at 25 °C are 0.8872 mPa·s and 1.330, respectively. The value of the viscosity must be adjusted when tests are not performed at 25 °C.

CLS (turbidity) method: Aliquots of ERM-FD101b shall be measured as-received, i.e. without dilution. The effective density of the silica particles is 2.0 g/cm^3. The temperature of the sample (for cuvette methods) or of the density gradient (for disc methods) shall be within the range [25 °C, 36 °C].

Electron microscopy method: The material should be transferred to a suitable grid/substrate; after drying, at least 250 discrete (non-overlapping) particles of the large particle population should be counted and measured. If necessary, ERM-FD101b can be diluted with purified water before transferring the particles to the grid/substrate.

Particle tracking analysis: ERM-FD101b should be diluted with purified water (filtered through a membrane with nominal pore size of 0.1 µm) to a particle concentration suitable for the user's instrument. Neither the as-received, nor the diluted silica suspension shall be treated by filtration, centrifugation or sonication. The measurement temperature shall be within the range [25 ± 5] °C.

Small-angle X-ray scattering: ERM-FD101b should be either analysed as-received, i.e. without dilution, or diluted in 2-fold in purified water. The measurement temperature shall be within the range [25 ± 5] °C.

9.4 Minimum sample intake

The minimum amount of sample to be used is for:

- CLS (turbidimetry): 100 µL;
- CLS (refractometry): 340 µL;
- DLS: 100 µL;
- EM: 2.5 µL of an as-received aliquot and analysis of at least 250 discrete particles;
- PTA: 1 µL. One shall analyse at least 500 tracks per measurement;
- SAXS: 20 µL.

9.5 Use of the certified value

The main purpose of this material is to assess the performance of instruments and/or methods that are used for measuring the size of nanoparticles. As any reference material, ERM-FD101b can also be used for control charts or validation studies.

Use as a calibrant

The certified values that have been assigned to the equivalent diameters are regarded as reliable estimates of the true values and ERM-FD101b can therefore be used for calibration purposes for EM and PTA methods. ERM-FD101b can also be used for the calibration of CLS instruments, provided that sufficient time is allowed after calibration for the sedimentation of the smaller particles of the 40 nm population, which otherwise would interfere with the signal of the first sample measured after calibration.

Comparing an analytical result with the certified value

A result is unbiased if the combined standard uncertainty of measurement and certified value covers the difference between the certified value and the measurement result (see also ERM Application Note 1, www.erm-crm.org [36].

For assessing the method performance, the measured values of the CRMs are compared with the certified values. The procedure is described here in brief:

- Calculate the absolute difference between mean measured value and the certified value (Δ_{meas}).
- Combine measurement uncertainty (u_{meas}) with the uncertainty of the certified value (u_{CRM}): $u_{\Delta} = \sqrt{u_{meas}^2 + u_{CRM}^2}$
- Calculate the expanded uncertainty (U_{Δ}) from the combined uncertainty ($u_{\Delta,}$) using an appropriate coverage factor, corresponding to a level of confidence of approximately 95 %
- If $\Delta_{meas} \leq U_{\Delta}$ no significant difference between the measurement result and the certified value, at a confidence level of about 95 % exists.

Use in quality control charts

ERM-FD101b can be used for quality control charts. Different CRM-units will give the same result as inhomogeneity was included in the uncertainties of the certified values.

10 Acknowledgements

The authors would like to acknowledge the support received from Jean Charoud-Got and John Seghers from the JRC, Directorate F related to the processing of this CRM and from Maria Contreras Lopez concerning the set-up of the required isochronous studies.

Furthermore, the authors would like to thank Katrien Busschots and Tsvetelina Gerganova (JRC, Directorate F) for the reviewing of the certification report, as well as the experts of the Certification Advisory Panel " Physicochemical-physical properties", Mark Gee (NPL, Teddington , UK), Jan Mast (CODA-CERVA, Brussels, BE) and Ludwig Niewöhner (Bundeskriminalamt, Wiesbaden, DE) for their constructive comments.

11 References

1 ISO Guide 34, General requirements for the competence of reference materials producers, International Organization for Standardization, Geneva, Switzerland, 2009

2 ISO Guide 35, Reference materials – General and statistical principles for certification, International Organization for Standardization, Geneva, Switzerland, 2006

3 ISO/IEC 17025:2005, General requirements for the competence of testing and calibration laboratories, International Organization for Standardization, Geneva, Switzerland, 2005

4 ISO/IEC Guide 98-3, Uncertainty of measurements –Part 3 : Guide to the expression of incertainty in measurement, (GUM 1995), International Organization for Standardization, Geneva, Switzerland, 2008

5 ISO/TS 80004-2, Nanotechnologies – Vocabulary – Part 2: Nano-objects, International Organization for Standardization, Geneva, Switzerland, 2015

6 Commission Recommendation of 18 October 2011 on the definition of nanomaterial, 2011/696/EU, 2011

7 M.N. Pons, H. Vivier, K. Belaroui, B. Bernard-Michel, F. Cordier, D. Oulhana, J.A. Dodds, Particle morphology: from visualisation to measurement, Powder Technol. 103 (1999) 44-57

8 ISO 13318-1, Determination of particle size distribution by centrifugal liquid sedimentation methods – Part 1: General principles and guidelines, International Organization for Standardization, Geneva, Switzerland, 2001

9 ISO 13318-2, Determination of particle size distribution by centrifugal liquid sedimentation methods – Part 2: Photocentrifuge method, International Organization for Standardization, Geneva, Switzerland, 2007

10 ISO 13318-3, Determination of particle size distribution by centrifugal liquid sedimentation methods – Part 3: Centrifugal X-ray method, International Organization for Standardization, Geneva, Switzerland, 2004

11 T. Detloff, T. Sobisch, D. Lerche, Particle size distribution by space or time dependent extinction profiles obtained by analytical centrifugation, Part. Part. Syst. Charact. 23 (2006) 184-187

12 H. Cölfen, W. Wohlleben, Analytical ultracentrifugation of latexes, In: L.M. Gugliotta, J.R. Vega (eds), Measurement of particle size distribution of latexes, Research Signpost, Kerala, India, 2010, pp 183-222

13 B.J. Berne, R. Pecora, Dynamic light scattering with applications to chemistry, biology, and physics, Dover Publications Inc., New York, USA, 2000

14 D.E. Koppel, Analysis of macromolecular polydispersity in intensity correlation spectroscopy: the method of cumulants, J. Chem. Phys. 57 (1972) 4814-4820

15 ISO 13321, Particle size analysis – Photon correlation spectroscopy, International Organization for Standardization, Geneva, Switzerland, 2001

16 ISO 22412, Particle size analysis – Dynamic light scattering (DLS), International Organization of Standardization, Geneva, Switzerland, 2008

17 S.W. Provencher, CONTIN: a general purpose constrained regularization program for inverting noisy linear algebraic and integral equations, Comput. Phys. Commun. 27 (1982) 229-242

18 S.W. Provencher, A constrained regularization method for inverting data represented by linear algebraic or integral equations, Comput. Phys. Commun. 27 (1982) 213-227

19 C. L. Lawson, R. J. Hanson, Solving least squares problems, Prentice-Hall Inc., Englewood Cliffs, New Jersey, USA, 1974

20 S. Twomey, Introduction to the mathematics of inversion of remote sensing and indirect measurements, Dover Publications Inc. New York, USA, 2002

21 ISO 13322-1, Particle size analysis – Image analysis methods – Part 1: Static image analysis methods, International Organization for Standardization, Geneva, Switzerland, 2004

22 P.-J. De Temmerman, E. Van Doren, E. Verleysen, Y. Van der Stede, M.A.D. Francisco, J. Mast, Quantitative characterization of agglomerates and aggregates of pyrogenic and precipitated amorphous silica nanomaterials by transmission electron microscopy, J. Nanobiotech. 10 (2012) 24, 11p

23 P.-J. De Temmerman, J. Lammertyn, B. De Ketelaere, V. Kestens, G. Roebben, E. Verleysen, J. Mast, Measurement uncertainties of size, shape, and surface measurements using transmission electron microscopy of near-monodisperse, near-spherical nanoparticles, J. Nanopart. Res. 16 (2014) 2177, 20p

24 S.B. Rice, C. Chan, S.C. Brown, P. Eschbach, L. Han, D.S. Ensor, A.B Stefaniak, J. Bonevich, A.E. Vladár, A.R.H. Walker, J. Zheng, C. Starnes, A, Stromberg, J. Ye, E.A. Grulke, Particle size distributions by transmission electron microscopy: an interlaboratory comparison case study, Metrologia 50 (2013) 663-678

25 O. Glatter, O. Kratky, Small angle X-ray scattering, Academic Press, London, UK, 1982

26 A. Guinier, G. Fournet, Small angle scattering of X-rays, Wiley, New York, USA, 1955

27 O. Glatter, A new method for the evaluation of small-angle scattering data, J. Appl. Crystallogr. 10 (1977) 415-421

28 ISO 17867, Particle size analysis – Small-angle X-ray scattering, International Organization for Standardization, Geneva, Switzerland, 2015

29 T.P.J. Linsinger, J. Pauwels, A.M.H. van der Veen, H. Schimmel, A. Lamberty, Homogeneity and stability of reference materials, Accred. Qual. Assur. 6 (2001) 20-25

30 A. Lamberty, H. Schimmel, J. Pauwels, The study of the stability of reference materials by isochronous measurements, Fres. J. Anal. Chem. 360 (1998) 359-361

31 A. Braun, K. Franks, V. Kestens, G. Roebben, A. Lamberty, T. Linsinger, Certification of equivalent spherical diameters of silica nanoparticles in water – Certified reference material ERM-FD100, EUR Report 24620 – European Union, Luxembourg - 2011 – ISBN 978-92-79-18676-9

32 K. Franks, A. Braun, V. Kestens, G. Roebben, A. Lamberty, T. Linsinger, Certification of the equivalent spherical diameters of silica nanoparticles in aqueous solution – Certified reference material ERM-FD304, EUR Report 25018 – European Union, Luxembourg - 2012 – ISBN 978-92-79-21866-8

33 T.P.J. Linsinger, J. Pauwels, A. Lamberty, H. Schimmel, A.M.H. van der Veen, L. Siekmann, Estimating the Uncertainty of Stability for Matrix CRMs, Fres. J. Anal. Chem. 370 (2001) 183-188

34 H. Woehlecke, T. Detloff, K. Franks, V. Kestens, G. Roebben, D. Lerche, In-situ determination of the effective particle density of suspended colloidal silica particles by means of analytical centrifugation, International Congress on Particle Technology (PARTEC), Nuremberg, Germany, 23-25 April 2013

35 ISO 9276-2, Representation of results of particle size analysis – part 2: Calculation of average particle sizes/diameters and moments from particle size distributions, International Organization for Standardization, Geneva, Switzerland, 2014

36 T. Linsinger, ERM Application note 1, www.erm-crm.org, last accessed 25/1/2016

37 V. Kestens and G. Roebben, Certification of equivalent diameters of a mixture of silica nanoparticles in aqueous solution : ERM-FD102, EUR 26656 – European Union, Luxembourg - 2014 – ISBN 978-92-79-38396-0

38 V. Kestens, V.A. Coleman, P.-J. De Temmerman, C. Minelli, H. Woehlecke, G. Roebben, Improved metrological traceability of particle size values measured with line-start incremental centrifugal liquid sedimentation, accepted for publication in Langmuir (2017), DOI: 10.1021/acs.langmuir.7b01714

39 CIPM, Report of the 96th meeting (2007) – BIPM, Paris, FR

40 S. D. Duke, E. B. Layendecker, Internal standard method for size calibration of sub-micrometer spherical particles by electron microscope, Technical Note TN-010.3, Thermo Fisher Scientific, Fremont, CA, USA, 2009

Annexes

Annex A: Results of the homogeneity measurements

Fig. A1 and Fig. A2 show the averages of the replicates measured per ampoule and their 95 % confidence intervals (error bar). These confidence intervals are based on the expanded measurements uncertainties *(k = 2)* of the DLS (cumulants method) and line-start CLS (disc centrifuge) methods operated in repeatability conditions, as obtained during in house method validation studies. Absolute values do not necessarily agree with the certified values due to potential laboratory bias, but this is irrelevant for the evaluation of homogeneity.

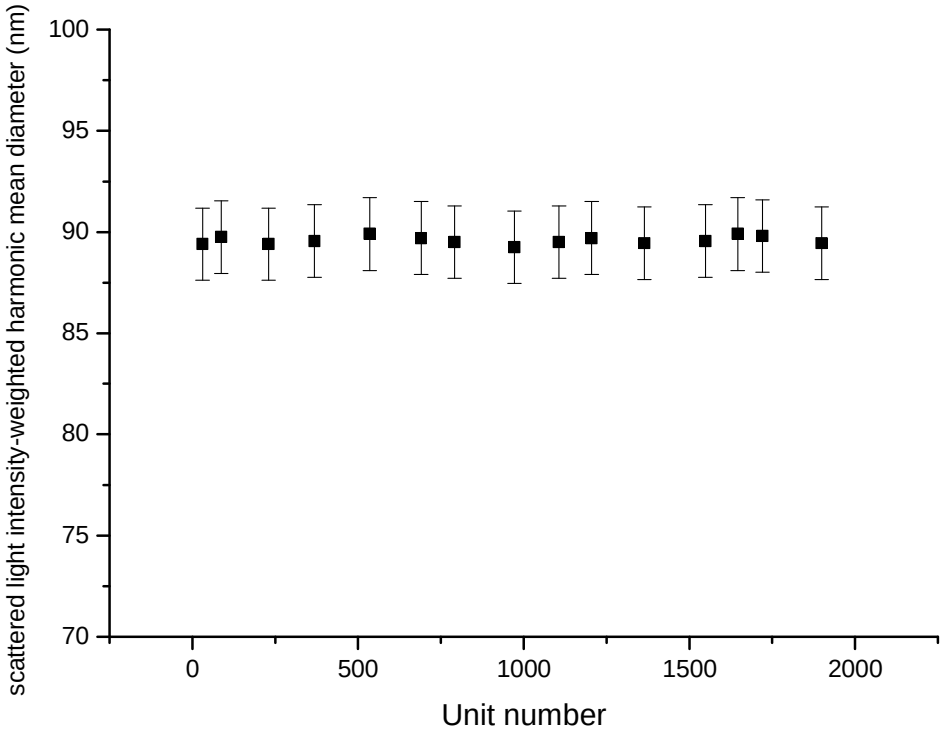

Fig. A1 Homogeneity data (average results of two replicates) of ERM-FD101b; DLS (cumulants method) scattered light intensity-weighted harmonic mean particle diameter; error bars correspond to the expanded measurement uncertainties *(k = 2)* for use of the method in repeatability conditions.

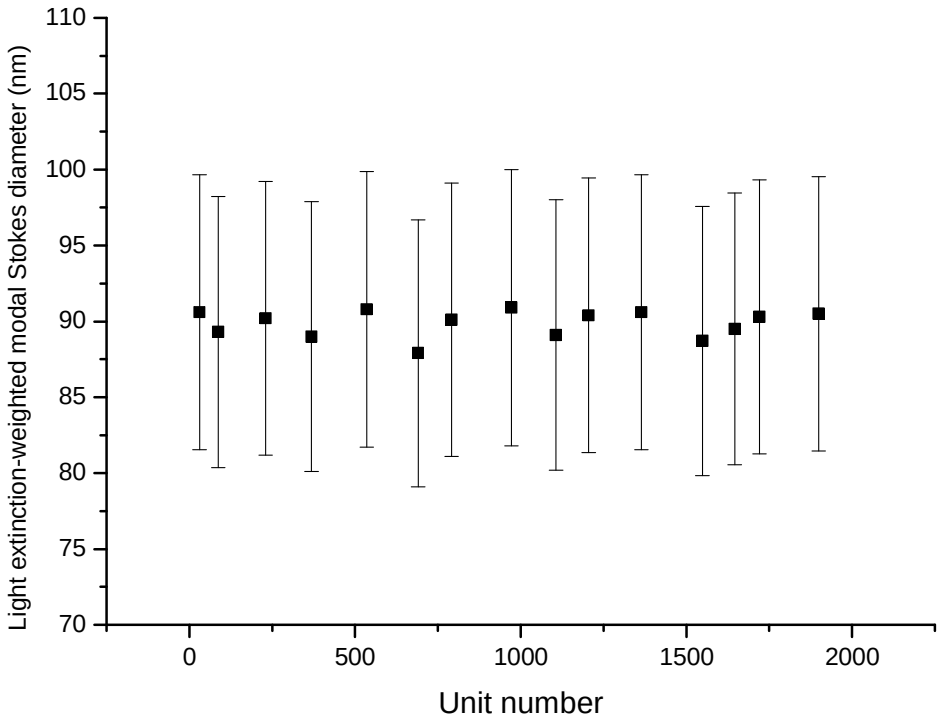

Fig. A2 Homogeneity data (average results of three replicates) of ERM-FD101b; line-start CLS (disc centrifuge) light extinction-weighted modal Stokes particle diameter; error bars correspond to the expanded measurement uncertainties *(k* = 2*)* for use of the method in repeatability conditions.

Annex B: Results of the short-term stability measurements

Graphs depicted in Fig. B1 and Fig. B2 show the short-term stability data as obtained with DLS (cumulants method) and with line-start CLS (disc centrifuge), respectively. Absolute values do not necessarily agree with the certified values due to potential laboratory bias, but this is irrelevant for the evaluation of the stability.

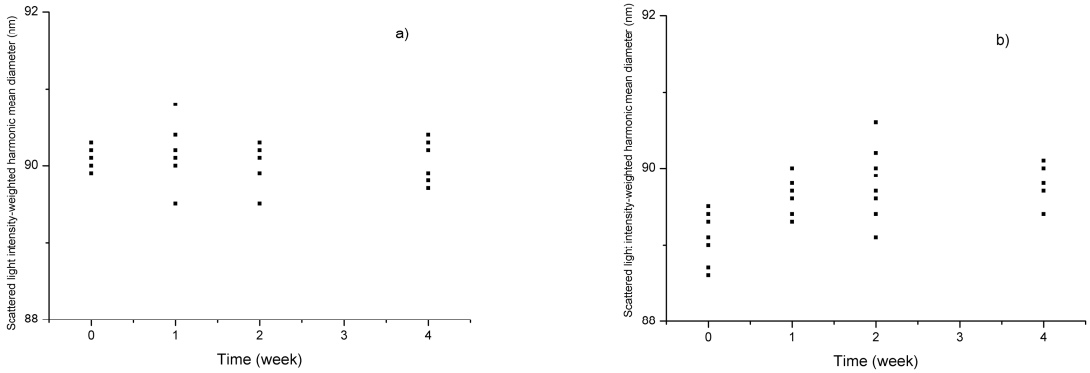

Fig. B1 Short-term stability data (results of individual replicates) of ERM-FD101b; DLS (cumulants method) results (scattered light intensity-weighted harmonic mean particle diameter), when stored several weeks at 4 °C (a) and 60 °C (b). Results at time point 0 weeks correspond to units that were stored at the reference temperature of 18 °C.

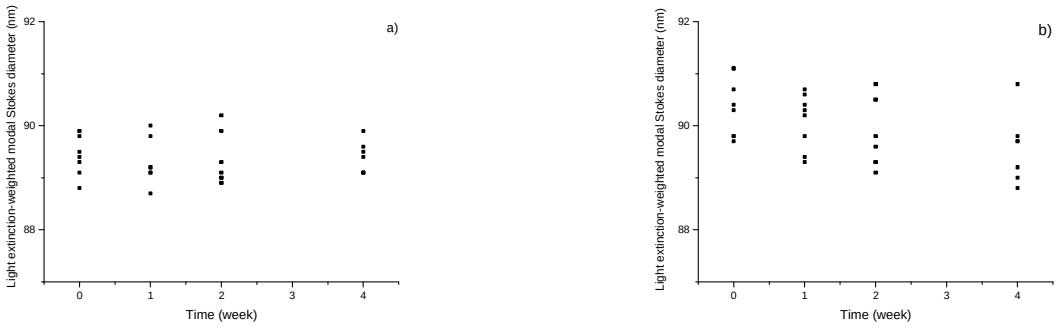

Fig. B2 Short-term stability data (results of individual replicates) of ERM-FD101b; line-start CLS (disc centrifuge) light extinction-weighted modal Stokes' particle diameter, when stored several weeks at 4 °C (a) and 60 °C (b). Results at time point 0 weeks correspond to units that were stored at the reference temperature of 18 °C.

Annex C: Results of the long-term stability measurements

Fig. C1 and C2 show the long term stability data obtained with DLS (cumulants method) and line-start CLS (disc centrifuge), respectively. Absolute values do not necessarily agree with the certified values due to potential laboratory bias, but this is irrelevant for the evaluation of stability.

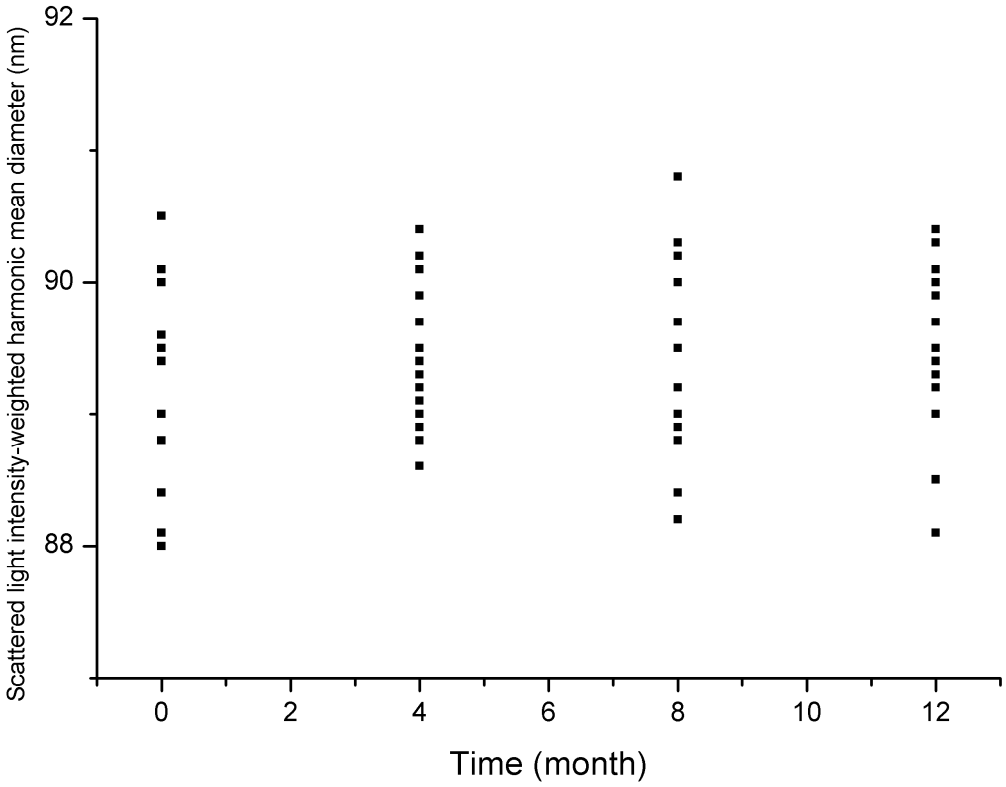

Fig. C1 Long-term stability data (results of individual replicates) of ERM-FD101b; DLS (cumulants method) results (scattered light intensity-weighted harmonic mean particle diameter), when stored several months at 18 °C. Results at time point 0 months correspond to units that were stored at the reference temperature of 4 °C.

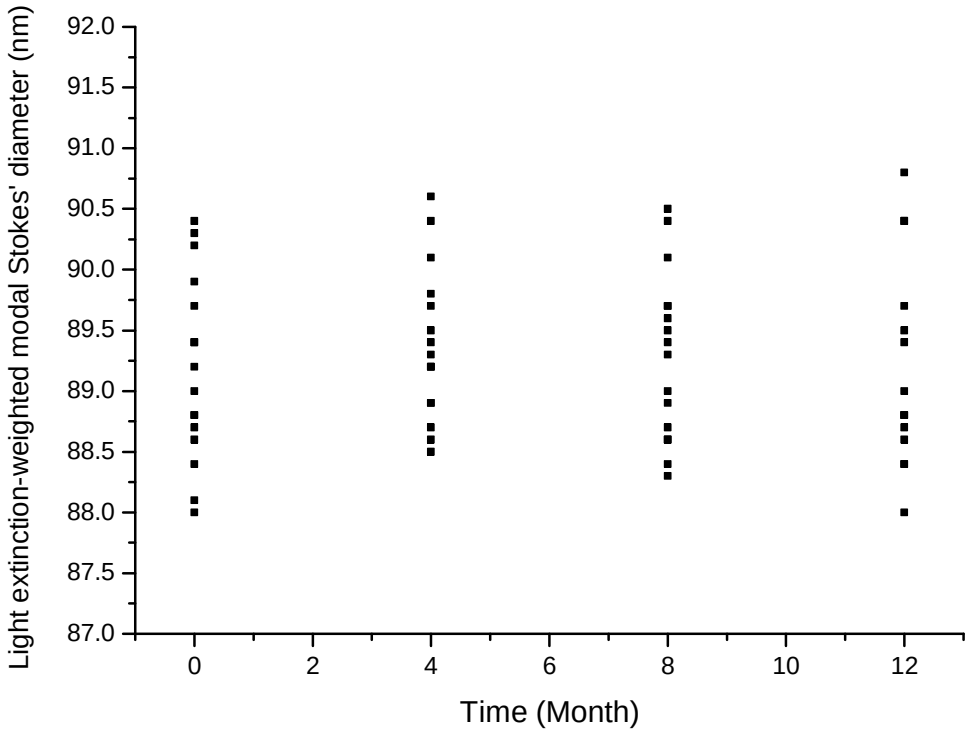

Fig. C2 Long-term stability data (results of individual replicates) of ERM-FD101b; line-start CLS (disc centrifuge) light extinction-weighted modal Stokes' particle diameter results, when stored several months at 18 °C. Results at time point 0 months correspond to units that were stored at the reference temperature of 4 °C.

Annex D: Summary of methods used in the characterisation study

Table D.1 Centrifugal liquid sedimentation: relevant instrumental and method details (as reported by the participants)

Lab code	Instrument make	Type	Mode of operation	Rotational speed [rpm]	Type of optics	Laser wavelength [nm]	Density gradient		Sample volume [µL]	Calibrant		
							Type / Temperature	Concentration interval [g/kg]		Type	Particle density [g/cm^3]	Assigned modal value [nm]
L2	Disc Centrifuge DC24000 (CPS Instruments Inc.)	Disc	Line-start	20000	Turbidity	470	Sucrose 28 °C	0 to 80	200	PVC particles (CPS Instruments Inc.)	1.385	377
L5	Disc Centrifuge DC24000 (CPS Instruments Inc.)	Disc	Line-start	24000	Turbidity	470	Sucrose 30 °C	80 to 240	500	Silica microspheres (Duke Scientific)	1.83	490
L9	Disc Centrifuge DC24000 (CPS Instruments Inc.)	Disc	Line-start	20000	Turbidity	405	Sucrose 29.5 °C	40 to 120	100	PVC particles (CPS Instruments Inc.)	1.385	239
L14	LUMiSizer 651 (LUM GmbH)	Cuvette	Homogeneous	4000	Turbidity	470	n.a. 25 °C	n.a.	n.a	n.a.	n.a.	n.a.
L16	Disc Centrifuge DC24000 (CPS Instruments Inc.)	Disc	Line-start	22000	Turbidity	405	Sucrose (not reported)	80 to 240	300	PVC particles (CPS Instruments Inc.)	1.385	226

L17	LUMiSizer 651 (LUM GmbH)	Cu-vette	Homoge-neous	4000	Turbidity	470	n.a. 25 °C	n.a.	n.a	n.a.	n.a.	n.a.
L18	Optima XL-I (Beckman-Coulter)	Cu-vette	Homoge-neous	3000	Refractive index	675	n.a. 25 °C	n.a.	n.a	Counter balance cells	n.a.	n.a.
L20	Disc Centrifuge DC24000 (CPS Instruments Inc.)	Disc	Line-start	24000	Turbidity	405	Sucrose 36 °C	80 to 240	100	PVC particles (CPS Instruments Inc.)	1.385	263
L23	Disc Centrifuge DC20000 (CPS Instruments Inc.)	Disc	Line-start	20000	Turbidity	405	Sucrose 29 °C	20 to 80	300	PVC particles (CPS Instruments Inc.)	1.385	239
L28	Optima XL-I/ XL A (Beckman-Coulter)	Cu-vette	Homoge-neous	3000	Refractive index		n.a 25 °C	n.a.	340	Counter balance cells	n.a	n.a

n.a. = not applicable

Table D.2 Dynamic light scattering: relevant instrumental and method details (as reported by the participants)

Lab code	Instrument type / make	Method	Laser			Detector		Sample cell			Analysis type
			Source	Wave-length [nm]	Power [mW]	Type ‡	Angle [°]	Type	Cuvette dimension length [mm]	Aliquot volume [mL]	(in addition to the Cumulants method)
L1	Malvern Zetasizer Nano ZS	Correlation function analysis	He-Ne	633	4	APD	173	Quartz glass microcuvette	10	0.125	NNLS
L2	Malvern Zetasizer Nano ZS	Correlation function analysis	He-Ne	633	4	APD	173	Disposable polystyrene cuvette	10	1	NNLS GP
L3a	Malvern Zetasizer Nano ZS90	Correlation function analysis	He-Ne	633	n.a.	APD	90	Standard quartz glass cuvette	10	1	n. a.
L3 b	Malvern Zetasizer Nano ZS	Correlation function analysis	He-Ne	633	n.a.	APD	173	Standard quartz glass cuvette	10	1	n. a.
WhL 4	Malvern Zetasizer Nano ZSP	Correlation function analysis	He-Ne	633	10	APD	173	Disposable Polystyrene cuvette	10	1	NNLS MNM
L5	Coulter N4 PLUS Submicron Particle Sizer	Correlation function analysis	He-Ne	633	4	PMT	90	Disposable Polystyrene cuvette	10	1	CONTIN (SDP analysis)
L6	Coulter N4 PLUS Submicron Particle Sizer	Correlation function analysis	He-Ne	633	10	PMT	90	Disposable acrylic cuvette	10	3	CONTIN (SDP analysis)
L7	Horiba NanoPartica SZ-100Z	Correlation function analysis	Diode	532	10	PMT	90	Disposable plastic cuvette	10	1	n. a.
L8	Malvern Zetasizer Nano ZS	Correlation function analysis	He-Ne	633	4	APD	173	Disposable PMMA cuvette	10	1.5	NNLS
L9	Malvern Zetasizer Nano ZS	Correlation function analysis	He-Ne	633	4	APD	173	Disposable polystyrene cuvette	10	0.5	NNLS GP
L12	Malvern Zetasizer Nano ZS	Correlation function analysis	He-Ne	633	4	APD	173	Disposable polystyrene cuvette	10	3	NNLS
L13	Malvern Zetasizer Nano ZS	Correlation function analysis	He-Ne	633	4	APD	173	Disposable polycyclic olefin	10	0.1	NNLS MNM + Q-corrrection

L19	Malvern Zetasizer Nano ZS	Correlation function analysis	He-Ne	633	4	APD	173	Disposable polystyrene cuvette	10	1	NNLS MNM
L20	Malvern Zetasizer Nano ZS	Correlation function analysis	He-Ne	633	4	APD	173	Disposable polystyrene cuvette	10	1	NNLS MNM
L23	Malvern Zetasizer Nano ZS	Correlation function analysis	He-Ne	633	4	APD	173	quartz cuvette	10	1	NNLS GP
L24	HORIBA SZ-100 Nano Partica	Correlation function analysis	Diode	532	10	PMT	90	Disposable plastic cuvette	10	1.5	Inverse Histogram method
L27	NANOPHOX PARTICLE ANALYSER, NX0059	3D-cross-correlation function analysis	He-Ne	633	15	APD	90	Disposable acrylic cuvette	10	0.3	n.a.
L29	Malvern Zetasizer Nano ZS	Correlation function analysis	He-Ne	633	4	APD	173	Standard quartz glass cuvette	10	1	NNLS
L32	ALV-6010/160	3D-cross-correlation function analysis	YAG	532	500	Photo-diode	90	Disposable polystyrene Cuvette	10	2	n.a.
L36	NANOPHOX PCCS	3D-cross correlation function analysis	Diode	658	30	APD	90	Disposable acrylic cuvette	10	1	NNLS

n.a. = not available or reported by participant, ‡ APD: avalanche photodiode detector; PMT: photomultiplier tube; GP: General Purpose, regulariser 0.01; MNM : Multi Narrow Mode, regulariser 0.001

Table D.3 Electron microscopy: relevant instrumental and method details (as reported by the participants)

Lab code	Instrument type / Make	Acceleration voltage - SEM working distance	Magnification calibration - Metrological traceability	Specimen preparation	SEM electron detector type - TEM imaging mode	CCD camera type	Total sampled area [μm^2]	Image magnification [1000x]	Pixel size [nm]	Total # of particles counted	Image analysis software - Image analysis strategy	Bin size [nm]
L2	TEM Philips CM200	80 kV	Optical diffraction cross-grating (No. 607) with 2160 lines/mm and 463 nm line spacing (Ted Pella, Inc.) Reference polystyrene particles with certified mean diameters of 112 nm (S130-1), 305 nm (S130-5) and 1036 nm (S130-7) (Plano GmbH) Traceability statement not available	2.5 µL of the as-received suspension brought onto a Carbon-coated grid (Cu 200 mesh) and vacuum dried	Bright-field Condenser aperture n°4	Olympus SIS Mega-view II CCD Pixels 1k x 1k	0.935	78	0.84	6307	iTEM (Olympus Soft Imaging Solutions GmbH) Manual optimisation of image brightness /contrast, each particle was manually measured as a polygon clicking on the perimeter of the particles	2
L9a	SEM Zeiss Supra 40 Field Emission Gun SEM	10 kV Between 3 nm and 3.6 mm	Grid with 2160 lines/mm or a pitch spacing of 463 nm in both X and Y direction (Agar Scientific) Si specimen, RM8820 with line spacing of 201 nm (NIST)	10x to 500x diluted with ultrapure water 20 µL of the diluted solution brought on a 1 5Alcian blue modified 200 mesh carbon coated copper grid. Grid dried with compressed air	In-lens secondary electron 20 µm	n.a.	1250	100	1.8	18362	Zeiss SmartStich software. ImageJ v1.48 was used to crop the images to remove areas where overlap with others scans had occurred and remove the top part of the image where minor drift had occurred. Software Microsoft Excel 2010 and OriginPro 9.1 for data analysis	1

Lab code	Instrument type / Make	Acceleration voltage - SEM working distance	Magnification calibration - Metrological traceability	Specimen preparation	SEM electron detector type - TEM imaging mode	CCD camera type	Total sampled area [μm^2]	Image magnification [1000x]	Pixel size [nm]	Total # of particles counted	Image analysis software - Image analysis strategy	Bin size [nm]
L9b	SEM Zeiss Supra 40 Field Emission Gun SEM	10 kV Between 3 nm and 3.6	Grid with 2160 lines/mm or a pitch spacing of 463 nm in both X and Y direction (Agar) Si specimen, RM8820 with lines by 201 nm (NIST)	10 to 500x diluted with ultrapure water 20 µL of the diluted QCM\CRM solution on a Alcian blue modified 200 mesh carbon coated copper grid. Grid dried with compressed air	Scanning TEM diode detector	n.a.	1250	100	1.8	18362	Zeiss SmartStich software. Excel 2010 and OriginPro 9.1 for data analysis ImageJ v1.48 was used to crop the images to remove areas where overlap with others scans had occurred and remove the top part of the image where minor drift had occurred.	1
L10	TEM Tecnai G2 Spirit TEM (FEI, Eindhoven, The Netherlands)	120 kV	Optical diffraction cross-grating (S106) with 2160 lines/mm and 463 nm line spacing (Agar Scientific) Traceability statement not available	50 µL taken from the as-received material and 10x diluted with ultrapure water Alcian blue pre-treated Pioloform® carbon-coated grid (Cu 400 mesh) placed on a drop (15 µL) of diluted suspension, 10 min incubation, washed and air dried	Bright-field with objective aperture of 150 µm	Eagle CCD Bottom-mount Pixels 4k x 4k	93	13	0.82	13015	iTEM (Olympus Soft Imaging Solutions GmbH) and Sigmaplot® Manual grey-scale thresholding, and automated particle size analysis, lognormal fit using Fityk software Particles were detected based on their sphericity (>0.4) and convexity (>0.8)	1

Lab code	Instru-ment type / Make	Accele-ration voltage - SEM working distance	Magnification calibration - Metrological traceability	Specimen preparation	SEM electron detector type - TEM imaging mode	CCD camera type	Total sam-pled area [μm^2]	Image magnifi-cation [1000x]	Pi-xel size [nm]	Total # of parti-cles coun-ted	Image analysis software - Image analysis strategy	Bin size [nm]
L13	SEM FEI Helios Dual-Beam	5 kV 4 mm	NanoLatticeTM standard with nominal 100 nm pitch (VLSI Standards, Inc.) Pitch size standard calibrated on metrological AFM, pitch value of 99.9 nm ± 1.5 nm (k = 2) traceable to SI Unit, metre Magnification verified using 100 nm PSL spheres (NIST SRM 1963a)	Single-crystal silicon chips coated with poly-L-lysine. The substrates are incubated with 50 µL sample solution without dilution for 3 seconds, and then washed with DI water and dried with air.	Standard SE detector	n.a	7 to 315	65	1.9	8690	ImageJ v1.47 Manual setting of contrast and brightness Binarisation by baseline thresholding and automated particle size analysis and lognormal fit, particles touching each other or cut by image border were excluded	<0.1
L15a	TEM Carl Zeiss Libra 120	120 kV	Optical diffraction cross-grating (S106) with 2160 lines/mm and 463 nm line spacing) (Plano GmbH) Traceability statement not available	Dilution of the Sample 10 to 20x diluted with ultrapure water 2 µL of the diluted suspension brought onto a carbon-coated grid (Cu 400 mesh) and air dried in a clean room	Bright-field with objective aperture of 30 µm	TRS slow scan CCD Pixels 2k x 2k	500	20	0.7	6198	iTEM (Olympus Soft Imaging Solutions GmbH) Manual grey-scale thresholding, touching particles were manually excluded, particle sizes were automatically measured. No image filter was used	0.1

Lab code	Instrument type / Make	Acceleration voltage - SEM working distance	Magnification calibration - Metrological traceability	Specimen preparation	SEM electron detector type - TEM imaging mode	CCD camera type	Total sampled area [μm^2]	Image magnification [1000x]	Pixel size [nm]	Total # of particles counted	Image analysis software - Image analysis strategy	Bin size [nm]
L15b	SEM Carl Zeiss Neon-40-EsB	20 kV 5 mm	Calibration sample with Series No. IMS-HR 083641-01380 from Carl Zeiss Microscopy GmbH. Deviation: specified < 3 %, measured 1 %.	Dilution of the Sample 10 to 20x diluted with ultrapure water 2 µL of the diluted suspension brought onto a carbon-coated grid (Cu 400 mesh) that was placed on a carbon pad and air dried in a clean room	In-lens SE, aperture of 30 µm	n.a.	500	100	1.2	6336	iTEM and ImageJ Manual grey-scale thresholding, touching particles were manually excluded, particle sizes were automatically measured. Image filters were not used	0.1
L20	TEM JEOL 2100	100 kV	NIST RM 8013	1:800 dilution with 0.1 µm filtered ultrapure water (18.2 MΩ.cm) 6 µL of the diluted suspension drop cast onto a carbon coated grid (Cu 400 mesh), > 6 hr drying in cytotoxic cabinet	Bright-field with objective aperture of 40 µm	Gatan Ultrascan 1000 CCD Pixels 2k x 2k	168 to 341	10	1 to 2	8945	ImageJ version 1.45s Semi-automated particle detection, manual setting of contrast and brightness, 7x7 filter, particles touching or cut by field of view excluded from analysis	1.0

Lab code	Instrument type / Make	Acceleration voltage - SEM working distance	Magnification calibration - Metrological traceability	Specimen preparation	SEM electron detector type - TEM imaging mode	CCD camera type	Total sampled area [μm^2]	Image magnification [1000x]	Pixel size [nm]	Total # of particles counted	Image analysis software - Image analysis strategy	Bin size [nm]
L27a	TEM LIBRA 200 FE (Zeiss)	200 kV	Mag*I*Cal single-crystal silicon reference standard (Technoorg-Linda Ltd.) Traceable to SI Unit, metre, through interplanar lattice spacing of a silicon crystal	Dilution 50x with ultrapure water	Bright-field with objective aperture of 500 µm	Telescopic SSCCD Camera (Gatan 894.20p.2)		20	0.6	6389	The Buehler Omnimet image system was used for image processing and diameter measurement. The particles were separated manually with thresholds and finally the diameters are derived from the area of the particles.	1
L27b	SEM Carl Zeiss Ultra 55 FE	5 kV 4.5 mm	400 nm pitch spacing standard (Chinese Academy of Sciences) Pitch size standard SI traceably calibrated on metrological AFM	Dilution 100x with ultrapure water	30 µm aperture size	n.a.		30	3.7	6720	Image J software for image processing and diameter measurements. The particles were separated automatically with threshold methods and the diameters are derived from the areas of the particles. The modal diameter were estimated by fitting the histogram with a normal distribution	1

Lab code	Instrument type / Make	Acceleration voltage - SEM working distance	Magnification calibration - Metrological traceability	Specimen preparation	SEM electron detector type - TEM imaging mode	CCD camera type	Total sampled area [μm^2]	Image magnification [1000x]	Pixel size [nm]	Total # of particles counted	Image analysis software - Image analysis strategy	Bin size [nm]
L33 a	SEM JEOL JSM-6500F	20 kV	Agar Scientific Ltd. S1930 Silicon Test Specimen Certified Specimen No. A877	Sample was used as received. The TEM grids (copper, 200 mesh, carbon only film) was dipped in silica solution	Lens detector	n.a	11.8 to 18.2	100	0.9	6154	NIH ImageJ software. Touching particles were measured only if their complete circumference was clearly visible. Microsoft Excel was used to determine the area equivalent circular diameter, median and modal particle diameters, and generate particle size distributions. Brightness, contrast and grayscale were not adjusted for particle sizing. Brightness,contrast and grayscale were not adjusted for CRM particle sizing	
L33 b	TEM Philips CM120	100 kV	Mag-i-Cal calibration standard Traceable to SI Unit, metre, through interplanar lattice spacing of a silicon crystal	The TEM grids (copper, 200 mesh, carbon only film) was dipped in the as received silica solution	Lens detector	Scientific Instruments & Applications (SIA) 2k by 2k CCD camera	12 to 17.1	100	0.5	6177	NIH ImageJ software. Touching particles were measured only if their complete circumference was clearly visible. Microsoft Excel was used to determine the area equivalent circular diameter, median and modal particle diameters, and generate particle size distributions. Brightness, contrast and grayscale were only adjusted for particle sizing of QCM.	

Lab code	Instrument type / Make	Acceleration voltage - SEM working distance	Magnification calibration - Metrological traceability	Specimen preparation	SEM electron detector type - TEM imaging mode	CCD camera type	Total sampled area [μm^2]	Image magnification [1000x]	Pixel size [nm]	Total # of particles counted	Image analysis software - Image analysis strategy	Bin size [nm]
L34	SEM Zeiss Leo Supra 35 VP	30 kV 5mm	Calibration with calibrated artefact containing a 2D grating with a pitch of 144 nm and 700 nm Traceable calibration of the grating by laser diffractometry	Sample was used as receveid. 1 to 2 µL on 200 mesh TEM grids covered with carbon film (type S160 from Plano GmbH)	Five solid state electron detectors, Four detectors used as dark field detectors and the fifth one use for bright-field imaging (transmission mode)	n.a	329 to 3848	100	4.5	9058	Image Analysis in several steps : Global thresholding Iterative determination of threshold (and size) Interpolation of the image and final size determination Particle selection (only particle in the size range 60-100 nm with circularity above 0.8 were analysed) statistics	1 and 2
L29	TEM Tecnai G2 20 S-TWIN, FEI	200 kV	Calibration with gold standard sample with grid (300 meshes). Calibration at low magnification with grId and Au lattice at high magnification grid	1000x dilution with ultrapure water 3 µL of diluted sample copper grid with carbon film, 200 meshes	Bright field	200 KV, CCD camera,	1.295 per sample	13.8	1.1	8066	Image J treatment of particles cut by the measurement frame (ISO 13322-1:2004)	1

Table D.4 Particle tracking analysis: relevant instrumental and method details (as reported by the participants)

Lab code	Instrument type / make	Aliquot preparation	Laser			Camera type	Aliquot volume [mL]	Measurement duration [s]	Camera shutter	Analysis software	Bin width [nm]	Calibration or PQ
			Source	Wavelength [nm]	Power [mW]							
L9	NanoSight LM10 HSB	1 µL diluted in ultrapure water 1:5000 (final dilution)	Diode	640	40	CCD	0.25	60	n.a	NTA 2.3	n.a	By manufacturer
L10	NanoSight LM10 HSBF	Aliquots were prepared in a class II cabinet. Test portions were taken from the ampoule with a clean pipette using a new tip for each aliquot. 50 µL of the as-received material was diluted in 450 µL MilliQ water (filtered through 0.1 µm filter), 20 000x dilution	Diode	405	60	sCMOS	0.25	60	1000	NTA 2.3	n.a	QC with NIST RM 8012-8013
L11	NanoSight NS500	Test portions taken from the ampoules were 6000x diluted in pre-filtrated ultrapure water that was passed through a filter with nominal pore sizes of 0.1 µm.	Diode	405	< 60	EMCCD	0.25	60	n.a.	NTA 3.0	n.a.	QC with NIST RM 8012
L20	NanoSight LM14	The sample was diluted (1000x to 2000x) by ultrapure water. Sample preparation was done in a cytotoxic cabinet fitted with a high-efficiency particulate air (HEPA) filter.	Diode	532	50	sCMOS	0.5	60	5	NTA 2.3	n.a.	Calibration with Thermo-Scientific PSL (100 nm)
L27	NanoSight LM20	Original sample dilute 2500 to 5000x in ultrapure water Sample prepare in clean room (class 6)	laser	638	40		0.25	60	n.a	NTA 2.3	n.a	Calibration with Thermo-Scientific PSL 3010 (100 nm)

L30	NanoSight NS500	10 µL sample is diluted 100 x with ultrapure water (filtered on 0.1 µm filter). 20 µL of this first dilution is diluted in 1980 µL ultrapure water to reach a 10 000 X final dilution.	laser	532		EMCCD	0.25	60	33	NTA 2.3	n.a	QC with Thermo-Scientific PSL 3100A, 3200A
L31	NanoSight LM10 HSB	Dilution 10000x with ultrapure water	Diode	405	<40	sCMOS	0.5	60	n.a	NTA 3.0	n.a	QC with Thermo-Scientific PSL 3050A, 3100A, 3200A

Table D.5-1 Small-angle X-ray scattering (SAXS): relevant instrumental details (as reported by the participants)

Lab code	Base instrument	X-ray generator / source	X-ray beam / optics	Detector	Aliquot preparation / Temperature	Sample holder / container	Half of the scattering angle range [°]	Aliquot volume [µL]
L21	X'Pert PRO (PANalytical), Expert SAXS camera	X-ray tube, Cu-Kα	Line focus, with elliptical X-ray mirror / monochromator	PIXcel linear, solid state detector (PANalytical)	1 part sample / 2 parts ultrapure water / 24 °C	Disposable Mark tubes (quartz glass)	-0.10 to 4	30
L22	BESSY synchrotron	Synchroton radiation (photon energy 6000 eV)	4-crystal monochromator, pinhole collimation (0.5 x 0.5 mm^2)	Pilatus 1M (Dectris)	As received / 25 °C	Borosilicate capillary	0.037 to 1.6	20
L25	SAXSpace (Anton Paar)	X-ray tube IDE 3003, Cu-Kα, 40 kV / 50 mA (General Electric)	Line collimation	Mythen 1k, strip size 50 µm	As received / 25 °C	Quartz capillary	0.03 to 2.84	25
L26	CREDO	Microfocus X-ray tube, GeniX3D Cu ULD, Cu-Kα (Xenocs)	Parabolic X-ray mirror / monochromator, pinhole collimation	Pilatus-300k (Dectris)	As received / 25 °C	Capillary	0.031 to 1.31	20
L35	SAXSess (Anton Paar)	X-ray tube, Cu-Kα, 2.2 kW (PANalytical)	Line collimation	1D diode array	As received / 23 °C	Flow-through capillary	0.025 to 1.40	20

Table D.5-2 SAXS - Guinier approximation: relevant instrumental and method details (as reported by the participants)

Lab code	Measured *q*-range [1/nm]	Largest measurable size according to ISO 17867* [nm]	*q*-range used for linear fit of the QCM data [1/nm]	*q*-range used for linear fit of FD101b data [1/nm]	Calculation of R_G
L21	[0.045, 2.8]	140	[0.065, 0.135]	[0.045, 0.061]	Fit part of Gaussian to I(q) (via linear fit in $\ln(I(q)) - q^2$ plot)
L22	[0.021, 0.87]	300	[0.05, 0.15]	[0.025, 0.041]	Fit part of Gaussian to I(q); iteratively over different *q*-ranges, until $q_{G,max} = 1.3/R_G$
L25	[0.021, 2]	300	[0.042, 0.07]	[0.042, 0.07]	Fit part of Gaussian to I(q) (via linear fit in $\ln(I(q)) - q^2$ plot)
L26	[0.044, 1.862]	143	[0.048, 0.080]	[0.044, 0.1]	Fit part of Gaussian to I(q) (via linear fit in $\ln(I(q)) - q^2$ plot)
L35	[0.03652, 2]	172	[0.036, 0.16]	[0.036, 0.070]	Fit of part of Gaussian to I(q)

Table D.5-3 SAXS - model fitting approach: relevant instrumental and method details (as reported by the participants)

Lab code	Name used by lab to describe method (reference)	Assumptions about particles	Assumptions about size distribution	Weighting	Averaging / calculation of mean/reported value	Transformed to other weighting(s)?
L21	in acc. with ISO 17867, 9.3, Model Fitting (using EasySAXS v 2.0 software, PANalytical)	Homogeneous spheres	Monomodal, Gaussian shaped, 100 size classes	Volume	Mode (R_{50}) of fitted Gaussian peak	Analytically, to intensity
L22	in acc. with ISO 17867, 9.3, Model Fitting	solid spheres	Bimodal (main mode Gaussian, 2nd mode lognormal)	Number	Mode of Gaussian peak	Analytically, to volume and intensity
L25	in acc. with ISO 17867, 9.3, Model Fitting	Homogeneous spheres	Multimodal (20 cubic splines used to fit data)	Separate fits for volume and intensity	Mode of peak in size distribution curve	-
L26	in acc. with ISO 17867, 9.3, Model Fitting	homogeneous spheres	Bimodal, Gaussian	Separate fits for Number, volume and intensity	Mode of Gaussian peak	-
L35	Model fit	spheres	Monomodal, Gaussian	Number	Mode of Gaussian peak	-

Table D.6 Asymmetrical flow field-flow fractionation: relevant instrumental and method details (as reported by the participant)

Lab code	Instrument type / make	Aliquot preparation	Measurement parameters	Calibration
JRC - Directorate F	AF2000 MF (Postnova Analytics GmbH, DE)	Test samples were diluted to 1 mg/mL using ultrapure water	0.2 min with a constant cross flow of 1.0 mL/min, 40 min with linearly decaying cross flow (1.0 mL/min to 0 mL/min), 5 min without cross flow	Polystyrene latex standards Thermofisher (3030A, 3040A, 3050A, 3080, 3100A, 3125A, 3150A)

Table D.7 Zeta potential, pH and electrolytic conductivity: relevant instrumental and method details (as reported by the participant)

Lab code	Physical property	Instrument type / make / specifications	Aliquot preparation	Instrument calibration	Sample holder	Aliquot volume [mL]
JRC - Directorate F	Zeta potential	Malvern Zetasizer Nano ZS Light source: He-Ne, Power 4 mW, Wavelength 633 nm, Detector: APD, 13° angle, Model: Smoluchowski	Test samples were analysed as-received. Before loading of the sample, the measurement cell was pre-rinsed with ethanol of analytical grade and abundantly rinsed with ultrapure water.	n.a.	Polycarbonate folded capillary cell with gold-plated beryllium/copper electrodes	0.75
JRC - Directorate F	pH	744 pH Meter (Metrohm AG) Solitrode electrode with Pt1000 temperature sensor (Metrohm AG)	Test samples were analysed as-received.	2-point calibration using buffer solutions (Metrohm AG) with nominal pH values of 9.00 ± 0.02 (art. no. 6.2305.030) and 4.00 ± 0.02 (art. no. 6.2305.010)	Measurement in ampule before sample uptake	n.a
JRC - Directorate F	Electrolytic conductivity	Malvern Zetasizer Nano ZS	Test samples were analysed as-received		Polycarbonate folded capillary cell with gold-plated beryllium/copper electrodes	0.75

Annex E: Results of the characterisation measurements

Annex E1: Results of the characterisation measurements – DLS

Table E1.1 – Scattered light intensity-weighted harmonic mean particle diameter obtained by DLS (cumulants method).

Lab - code	Replicate results [nm]									Mean [nm]	s [1)] [nm]	U [2)] [nm]
	1	2	3	4	5	6	7	8	9			
L2	90.7	90.6	90.6	90.6	90.1	90.3	90.9	90.7	90.7	90.6	0.2	1.6
L3 a	87.1	86.9	87.2	87.3	87.6	86.8	87.1	87.2	86.8	87.1	0.3	3.0
L3 b	90.0	89.5	89.5	89.9	90.0	90.0	89.3	89.0	89.3	89.6	0.4	3.0
L4	90.4	90.2	90.1	90.5	90.2	90.3	90.4	90.3	90.4	90.3	0.1	3.1
L5	95.3	90.8	90.2	91.4	90.8	90.6	91.5	90.7	92.1	91.5	1.5	8.2
L6	83.8	83.6	83.6	83.7	83.6	83.5	83.7	83.6	83.6	83.6	0.1	6.7
L7	90.6	88.5	89.0	88.5	89.2	88.5	90.1	89.7	88.8	89.2	0.8	17.8
L8	90.4	90.4	90.9	91.8	92.5	91.9	91.1	91.1	90.3	91.2	0.8	6.9
L9	91.1	90.6	91.4	89.9	91.0	91.2	91.2	91.3	91.3	91.0	0.5	4.0
L13	90.5	90.3	90.3	89.9	90.4	90.2	90.1	89.7	89.8	90.1	0.3	3.4
L19	90.3	90.3	90.9	90.6	90.5	91.0	91.2	91.0	91.2	90.8	0.4	1.5
L20	90.3	90.6	90.4	90.6	90.6	90.4	90.5	90.6	91.2	90.6	0.3	1.6
L23	90.1	89.6	89.5	90.0	90.2	90.3	89.8	88.8	90.1	89.8	0.5	1.8
L24	88.6	89.2	89.7	90.5	90.0	90.2	86.8	89.9	90.2	89.5	1.2	17.9
L27	89.9	88.3	89.9	89.4	89.9	88.6	89.2	88.3	89.2	89.2	0.7	4.5
L36	88.5	89.1	88.2	87.7	89.9	88.5	89.0	87.4	87.4	88.4	0.8	2.7
Results not used for certification												
L1	94.5	93.5	93.2	93.2	94.2	94.4	93.7	92.7	92.0	93.5	0.8	0.4
L12	90.4	90.0	90.3	90.2	91.0	90.4	89.7	89.6	89.7	90.1	0.4	2.5
L29	89.3	90.1	89.3	90.1	89.41	90.1	89.8	89.1	89.3	89.6	0.4	3.6
L32	86.9	87.1	87.1	87.9	88.3	87.9	87.5	87.8	87.6	87.6	0.4	1.8

[1)] Standard deviation of the mean aliquot results

[2)] Expanded uncertainty *(k* = 2*)* as reported by the participants

Table E1.2 – Scattered light intensity-weighted mean particle diameter obtained by DLS (distribution calculation methods)

Lab - code	Replicate results [nm]									Mean [nm]	s [1] [nm]	U [2] [nm]
	1	2	3	4	5	6	7	8	9			
L2	94.9	94.5	94.9	94.4	94.4	94.1	95.1	94.8	94.7	94.6	0.3	1.7
L4	91.9	91.8	91.9	91.9	92.1	92.0	92.0	92.2	92.1	92.0	0.1	3.1
L5	93.2*	91.2	90.8	92.1	89.2	90.7	93.9	90.4*	92.9	91.6	1.5	8.2
L8	94.5	94.5	95.2	96.3	96.9	96.6	95.6	95.5	94.4	95.5	0.9	7.3
L9	94.5	94.7	94.7	94.4	94.8	95.1	94.8	95.2	95.5	94.9	0.3	4.2
L13	90.4	90.1	90.2	89.9	90.3	90.1	90.0	89.6	89.6	90.0	0.3	3.4
L19	93.8	93.6	94.7	94.1	94.2	94.9	94.9	94.9	94.7	94.4	0.5	1.5
L20	91.7	91.9	91.6	92.0	91.6	91.6	92.3	92.5	94.2	92.2	0.8	1.7
L23	93.5	93.6	93.5	94.3	94.3	94.0	93.8	92.6	94.0	93.7	0.5	1.9
L24	94.9	94.5	94.9	94.4	94.4	94.1	95.1	94.8	94.7	94.6	0.3	19.0
L36	89.6	89.6	88.3	89.0	91.3	89.8	90.3	89.5	88.4	89.5	0.9	2.7
Results not used for certification												
L1	97.8	97.8	97.4	97.0	97.8	98.8	97.2	96.7	96.2	97.4	0.3	0.4
L12	94.0	94.2	94.8	94.2	94.8	94.3	94.8	94.6	95.6	94.6	0.3	1.9
L29	93.2	93.7	93.7	93.5	93.3	93.3	93.2	93.8	93.6	93.5	0.2	3.7

[1] Standard deviation of the mean aliquot results

[2] Expanded uncertainty *(k* = 2*)* as reported by the participants

* For these aliquots, only two replicates were used for the calculations of the mean. One replicate was removed after evaluation of the data.

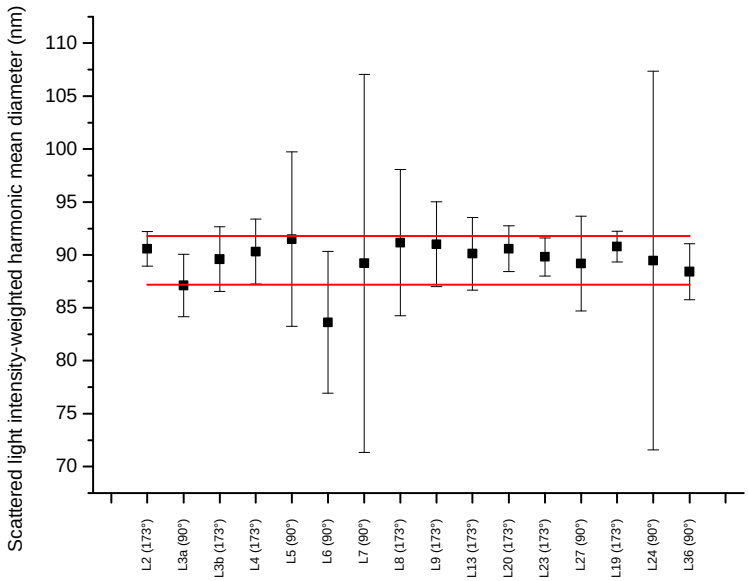

Fig. E1.1 Laboratory mean values (used for certification) of the DLS (cumulants method) light intensity-weighted harmonic mean particle diameters as obtained by 15 laboratories; error bars indicate the expanded ($k = 2$) measurement uncertainties as reported by the participants. The two horizontal lines reflect the certified range.

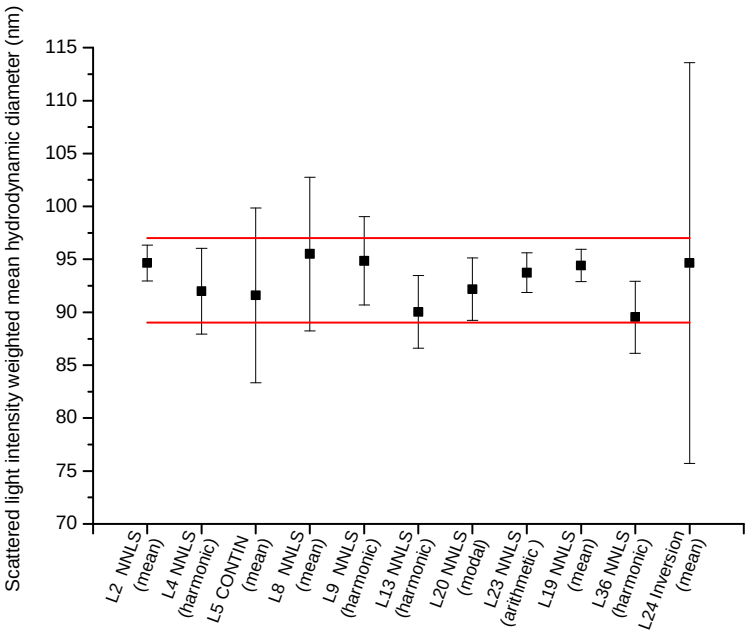

Fig. E1.2 Laboratory mean values (used for certification) of the DLS (distribution calculation methods) light intensity-weighted mean particle diameters as obtained by 11 laboratories; error bars indicate the expanded ($k = 2$) measurement uncertainties as reported by the participants. The two horizontal lines reflect the certified range.

Annex E2: Results of the characterisation measurements – CLS

Table E2.1 Light extinction-weighted modal Stokes particle diameter results obtained by CLS (turbidimetry)

Lab-code	Aliquot results [nm]						Mean [nm]	s [nm]	U [nm]
	1	2	3	4	5	6			
L2	87.1	87.3	86.8	87.3	86.6	87.1	87.0	0.2	9.1
L5	81.5	78.9	83.0	80.9	82.8	80.5	81.3	1.5	8.9
L9[a)]	87.7	87.5	87.8	87.9	87.7	87.8	87.7	0.1	10.5
L14	85.7	84.3	84.6	84.1	84.4	83.9	84.5	0.6	8.5
L16[b)]	92.3	92.0	92.9	91.9	93.1	92.3	92.4	0.4	3.7
L17	83.3	83.3	83.1	83.0	83.1	83.2	83.2	0.1	8.3
L20	87.9	87.5	88.0	87.6	87.9	87.7	87.8	0.2	6.5
L23	89.5	89.9	89.5	89.8	89.2	89.4	89.6	0.3	9.0

[a)] Laboratory L9 measured 4 aliquots per sample. Two replicates per sample (second and third measurements) were used for the calculations.

[b)] Laboratory L16 measured 6 aliquots per sample. Two replicates per sample were used for the calculations.

Table E2.2 Mass-weighted modal Stokes particle diameter results obtained by CLS (refractometry).

Lab-code	Aliquot results [nm]						Mean [nm]	s [nm]	U [nm]
	1	2	3	4	5	6			
L18	83.9	83.1	84.4	82.5	83.4	83.0	83.4	0.6	1.4
L28	84.7	84.3	84.7	84.3	85.3	84.7	84.7	0.3	3.1

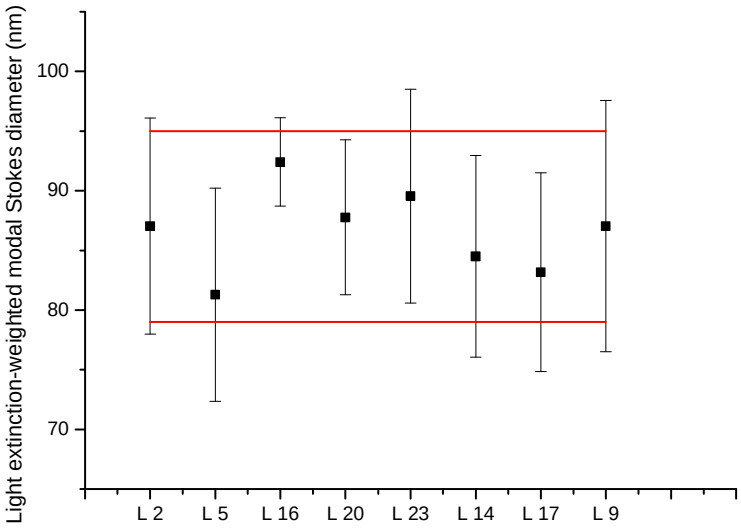

Fig E2.1 Laboratory mean values of the light extinction-weighted modal Stokes particle diameter obtained by 8 laboratories using CLS (turbidimetry); the error bars indicate the expanded (k = 2) measurement uncertainties as reported by the participants, the two horizontal lines reflect the certified range.

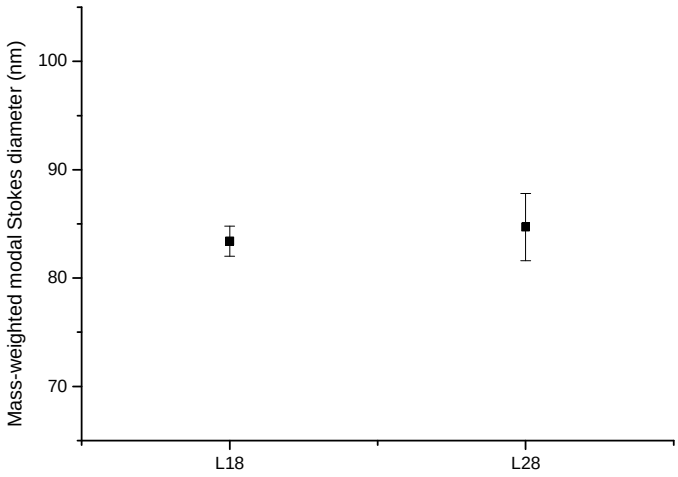

Fig E2.2 Laboratory mean values of the mass-weighted modal Stokes particle diameter obtained by 2 laboratories using CLS (refractometry); the error bars indicate the expanded (k = 2) measurement uncertainties as reported by the participants (L28) or calculated from the QCM results (L18).

Annex E3: Results of the characterisation measurements – EM

Table E3.1 Number-weighted modal area-equivalent particle diameter results obtained using EM

Lab - code	PSA Method	Replicate [nm]						Mean [nm]	s [nm]	U [nm]
		1	2	3	4	5	6			
L2	TEM	85.1	87.0	88.9	87.0	88.8	88.9	87.6	1.5	5.3
L10	TEM	85.5	85.6	85.8	85.8	85.8	85.5	85.7	0.2	3.9
L13	SEM	82.7	82.4	81.9	82.4	82.9	82.7	82.5	0.4	3.1
L15 a	TEM	82.7	82.8	83.8	83.0	84.4	83.5	83.3	0.7	5.0
L15 b	SEM	87.4	87.6	84.2	86.6	88.0	88.3	87.0	1.5	5.2
L20	TEM	81.0	81.0	82.0	82.0	84.0	84.0	82.3	1.4	11.5
L27 a	TEM	83.0	82.2	82.5	80.9	82.6	82.0	82.2	0.7	5.4
L27 b	SEM	83.0	80.7	81.6	83.1	79.5	81.8	81.6	1.4	3.6
L33 a	SEM	81.1	79.4	84.9	81.5	78.5	78.8	80.7	2.4	3.6
L33 b	TEM	81.4	81.9	83.8	81.7	82.2	80.6	81.9	1.1	2.8
L34	TSEM	85.9	85.1	84.7	85.0	86.0	86.5	85.5	0.7	5.1
Results not used for certification										
L9 a	TSEM	91.5	90.7	88.5	88.1	88.5	90.4	89.6	1.4	5.0
L9 b	SEM	85.5	88.5	88.1	85.1	87.5	83.5	85.9	1.7	10.6
L29	TEM	n. r.	n. r.	n. r.	n. r.	n. r.	n. r.	n. r.	n. r.	n. r.

n.r.: no results reported

Table E3.2 Number-weighted median area-equivalent particle diameter results obtained using EM

Lab - code	PSA Method	Replicate [nm]						Mean [nm]	s [nm]	U [nm]
		1	2	3	4	5	6			
L2	TEM	85.3	86.2	87.7	86.0	87.2	87.3	86.6	0.9	5.2
L 10	TEM	84.9	85.2	85.3	85.7	85.0	85.0	85.2	0.3	3.9
L 13	SEM	82.8	82.5	82.0	82.5	83.1	82.8	82.8	0.4	3.0
L15 a	TEM	83.0	81.6	84.1	82.8	83.1	84.3	83.2	1.0	5.0
L15 b	SEM	87.9	87.9	83.7	86.9	88.0	88.3	87.1	1.7	5.3
L 27 a	TEM	81.3	82.0	83.0	81.2	82.1	81.7	81.9	0.7	5.4
L 27 b	SEM	83.1	80.7	82.3	83.6	80.2	82.2	82.0	1.3	3.6
L 20	TEM	80.0	80.0	81.0	81.0	84.0	83.0	81.5	1.6	8.2
L 33 a	SEM	81.2	79.7	82.5	83.5	78.6	81.0	81.1	1.8	3.6
L 33 b	TEM	80.0	82.2	83.2	84.0	80.5	81.7	81.9	1.5	3.0
L34	TSEM	85.1	84.5	83.9	84.4	85.3	85.9	84.9	0.8	3.8
Results not used for certification										
L9	TSEM	89.3	89.0	87.0	85.7	86.3	89.0	87.7	1.6	4.9
L9	SEM	84.5	84.8	86.2	85.0	85.2	83.5	84.9	0.9	10.6
L29	TEM	81	78	87	80	76	76	79.7	4.1	15.9

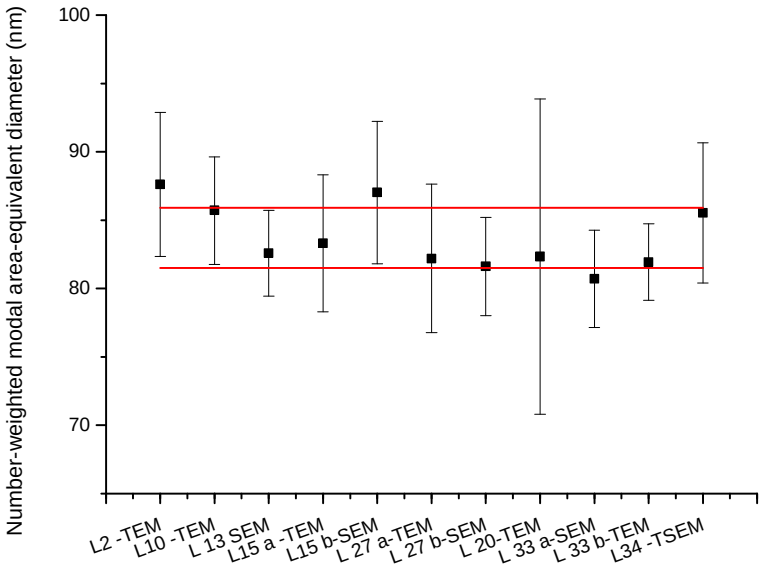

Fig E3.1 Laboratory mean values of the number weighted modal area-equivalent diameter as obtained by 9 laboratories using EM; the error bars indicate the expanded (k = 2) measurement uncertainties as reported by the participants, the two horizontal lines reflect the certified range.

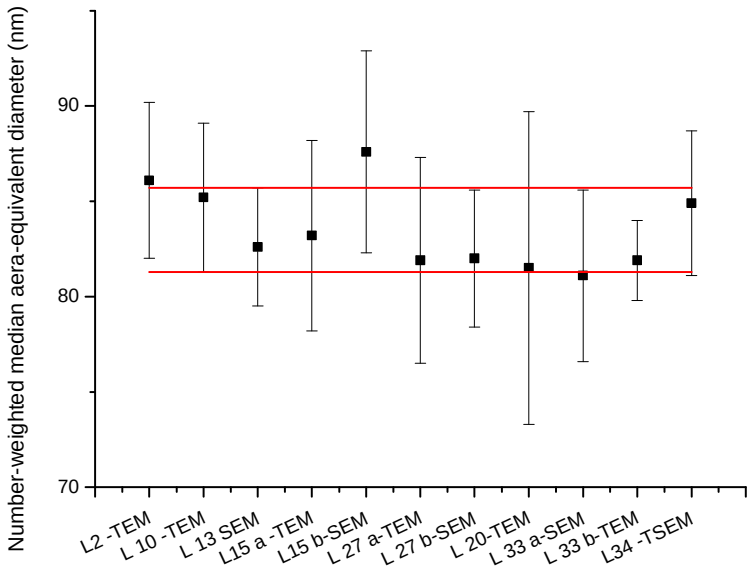

Fig E3.2 Laboratory mean values of the number weighted median area-equivalent diameter as obtained by 9 laboratories using EM ; the error bars indicate the expanded (k = 2) measurement uncertainties as reported by the participants, the two horizontal lines reflect the certified range.

Annex E4: Results of the characterisation measurements – PTA

Table E4.1 Number-weighted modal hydrodynamic particle obtained by PTA

Lab-code	Aliquot mean results [nm]									mean [nm]	s [nm]	U [nm]
	1	2	3	4	5	6	7	8	9			
L9	73.8	76.8	78.0	76.8	77.6	77.0	77.4	77.0	76.0	76.7	1.2	8.3
L10	82.5	81.8	83.3	84.2	83.5	79.5	81.5	81.3	83.2	82.3	1.4	9.2
L11	80.4	80.6	80.5	81.5	81.1	80.6	81.3	79.8	80.0	80.6	0.6	1.2
L20	84.4	82.0	85.2	84.0	83.2	84.6	82.8	83.4	84.0	83.7	1.0	7.0
L27	76.8	77.2	76.8	77.6	77.6	78.6	77.4	77.8	77.4	77.5	0.5	4.3
L30	87.6	85.0	85.4	83.6	86.8	84.2	85.4	83.6	84.2	85.1	1.4	1.7
L31	87.1	85.7	85.9	89.1	89.1	87.0	85.6	85.3	85.7	86.7	1.5	6.1

Table E4.2 Number weighted arithmetic mean hydrodynamic diameter obtained by PTA

Lab-code	Aliquot mean results [nm]									mean [nm]	s [nm]	U [nm]
	1	2	3	4	5	6	7	8	9			
L9	84.3	83.6	85.9	85.9	84.4	86.3	83.6	84.1	83.7	84.6	1.1	9.0
L10	87.2	86.7	88.4	90.6	88.4	86.1	88.3	87.1	87.6	87.8	1.3	9.8
L11	82.7	82.1	82.7	82.9	82.9	82.4	82.2	80.2	80.0	82.0	1.1	2.4
L20	93.0	92.1	95.2	94.8	92.6	94.5	96.0	94.3	96.4	94.3	1.5	17.4
L27	83.0	84.2	83.8	84.8	84.6	84.4	83.2	84.8	84.6	84.2	0.7	4.4
L30	90.8	89.8	89.0	89.6	91.0	88.0	90.2	87.8	88.4	89.4	1.2	1.4
L31	84.3	82.1	82.7	84.7	85.5	84.6	82.3	81.0	81.7	83.2	1.6	5.8

Table E4.3 Number weighted median hydrodynamic diameter obtained by PTA

Lab-code	Aliquot mean results [nm]									mean [nm]	s [nm]	U [nm]
	1	2	3	4	5	6	7	8	9			
L9	78.3	79.2	80.8	81.0	80.2	80.8	79.8	80.0	79.2	79.9	0.9	8.3
L10	83.8	83.2	84.3	86.0	84.7	81.8	83.2	83.0	84.0	83.8	1.2	9.4
L11	80.5	80.7	80.9	80.5	80.3	80.9	81.1	78.3	79.9	80.3	0.8	1.8
L20	87.3	86.4	88.8	88.2	86.7	88.3	89.0	88.3	88.4	87.9	0.9	9.1
L27	80.6	80.6	79.6	80.4	81.0	81.0	80.6	80.4	82.0	80.7	0.6	4.0
L30	87.8	86.8	86.2	86.2	88.0	85.4	87.2	85.2	85.4	86.4	1.1	1.2
L31	78.0	76.2	76.5	71.8	79.4	78.0	76.1	75.5	76.1	76.4	2.1	5.3

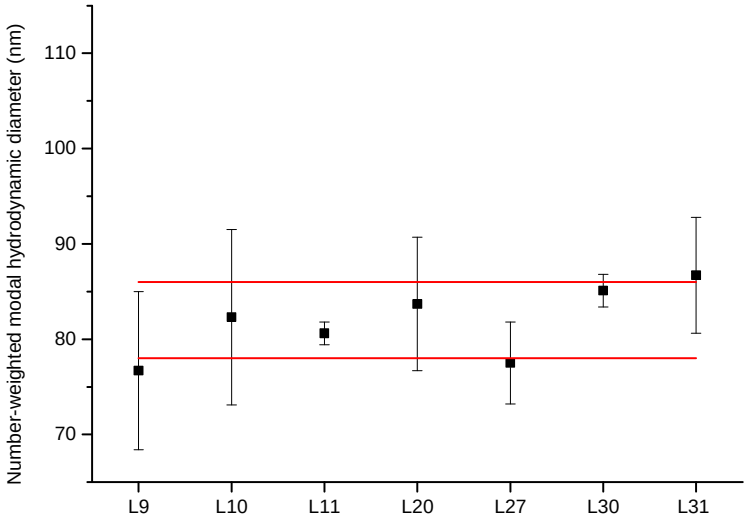

Fig. E4.1 Laboratory mean values of the number-weighted modal hydrodynamic diameters as obtained by 7 laboratories using PTA; error bars indicate the expanded (k = 2) measurement uncertainties as reported by the participants, the two horizontal lines reflect the certified range.

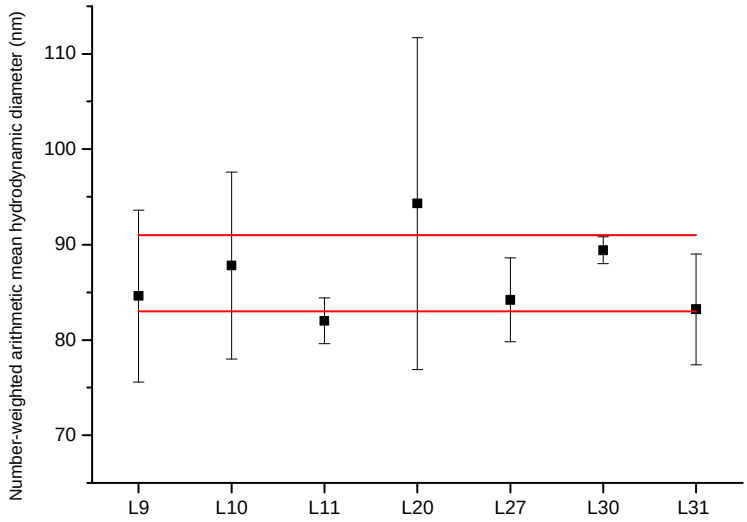

Fig. E4.2 Laboratory mean values of the number-weighted arithmetic mean hydrodynamic diameters as obtained by 7 laboratories using PTA; error bars indicate the expanded (k = 2) measurement uncertainties as reported by the participants, the two horizontal lines reflect the certified range.

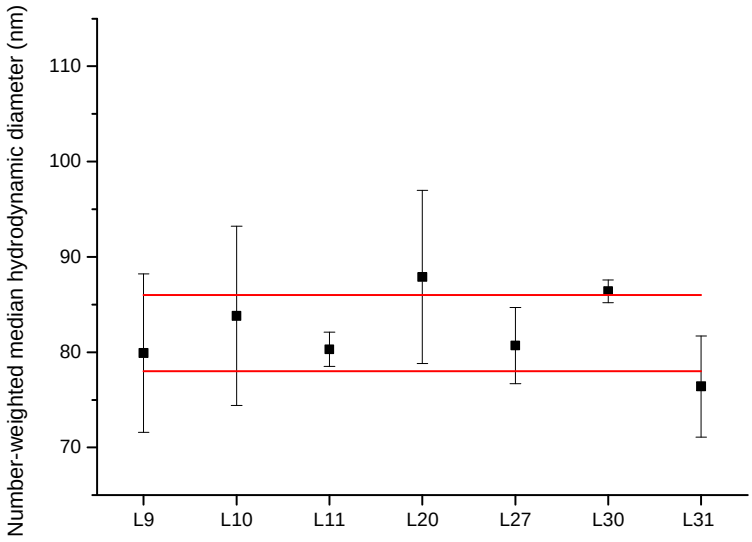

Fig. E4.3 Laboratory mean values of the number-weighted median hydrodynamic diameters as obtained by 7 laboratories using PTA; error bars indicate the expanded (k = 2) measurement uncertainties as reported by the participants, the two horizontal lines reflect the certified range.

Annex E5: Results of the characterisation measurements – SAXS

Table E5.1 (Volume)^2-weighted mean particle diameter (Guinier's approximation)

Lab code	Replicate [nm]						Mean [nm]	s [nm]	U [nm]
	1	2	3	4	5	6			
L21	86.8	86.5	85.9	86.3	86.5	86.9	86.5	0.4	4.2
L22	84.4	84.4	84.8	84.7	84.5	85.1	84.7	0.3	n.a.
L25	86.6	89.0	87.9	88.5	89.2	96.4	89.6	3.5	3.6
L26	90.8	90.8	90.7	90.9	90.9	90.8	90.8	0.1	7.4
L35	81.4	81.4	83.8	82.4	81.6	81.3	82.0	1.0	4.9

Table E5.2 Number-weighted modal particle diameter (model fitting)

Lab code	Replicate [nm]						Mean [nm]	s [nm]	U [nm]
	1	2	3	4	5	6			
L21	81.87	81.60	81.32	81.78	81.54	81.74	81.6	0.20	4.2
L22	81.09	81.09	81.12	81.12	81.10	81.10	81.1	0.01	1.3
L25	80	80.4	79.4	79.4	82.9	79.2	80.2	1.39	3.0
L26	80.7	80.7	80.9	80.9	80.8	80.9	80.8	0.10	3.4
L35	80.52	80.44	81.28	80.46	80.20	80.20	80.5	0.40	2.2

Table E5.3 Volume-weighted modal particle diameter (model fitting)

Lab code	Replicate [nm]						Mean [nm]	s [nm]	U [nm]
	1	2	3	4	5	6			
L21	82.68	82.41	82.13	82.59	82.35	82.55	82.5	0.20	4.2
L22	81.66	81.66	81.69	81.68	81.67	81.67	81.7	0.01	1.4
L25	83.3	82.1	81.3	81.34	83.4	80.48	82.0	1.17	3.0
L26	81.4	81.4	81.6	81.6	81.6	81.6	81.5	0.10	3.4
L35	80.94	80.86	81.70	80.88	80.62	80.62	80.9	0.40	2.2

Table E5.4 Scattered X-ray intensity-weighted modal particle diameter (model fitting)

Lab code	Replicate [nm]						Mean [nm]	s [nm]	U [nm]
	1	2	3	4	5	6			
L21	83.22	83.06	83.05	83.14	83.07	83.24	83.1	0.08	4.2
L22	82.22	82.22	82.24	82.24	82.23	82.23	82.2	0.01	1.5
L25	84	83	82.8	83.46	83.6	83.26	83.4	0.43	3.0
L26	82.2	82.1	82.3	82.2	82.3	82.3	82.2	0.08	3.4
L35	81.36	81.28	82.12	81.30	81.06	81.06	81.4	0.39	2.2

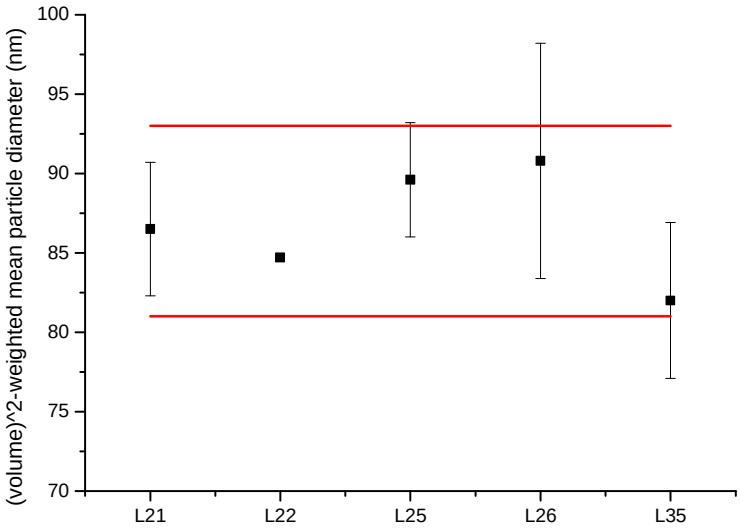

Fig. E5.1 Laboratory mean values of the (volume)^2-weighted-mean particle diameters as obtained by 5 laboratories using SAXS (Guinier approximation). The error bars indicate the expanded (k = 2) measurement uncertainties as reported by the participants, the two horizontal lines reflect the indicative range.

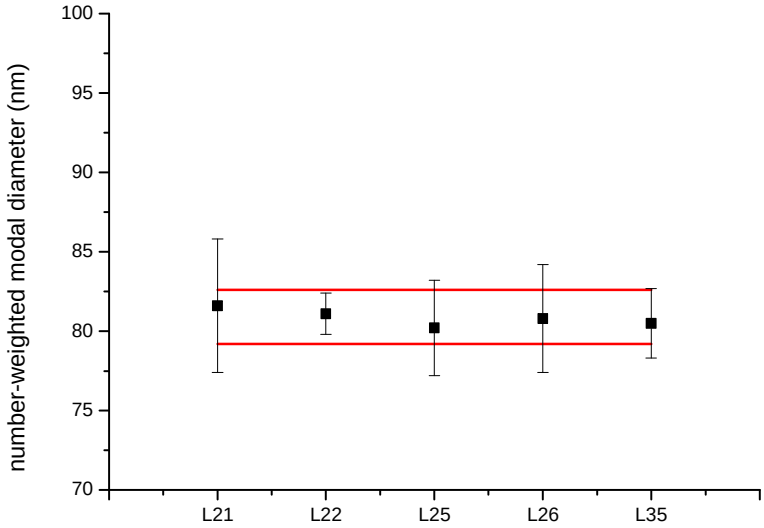

Fig. E5.2 Laboratory mean values of the number-weighted-modal particle diameters as obtained by 5 laboratories using SAXS (model fitting approach). The error bars indicate the expanded (k = 2) measurement uncertainties as reported by the participants, the two horizontal lines reflect the certified range.

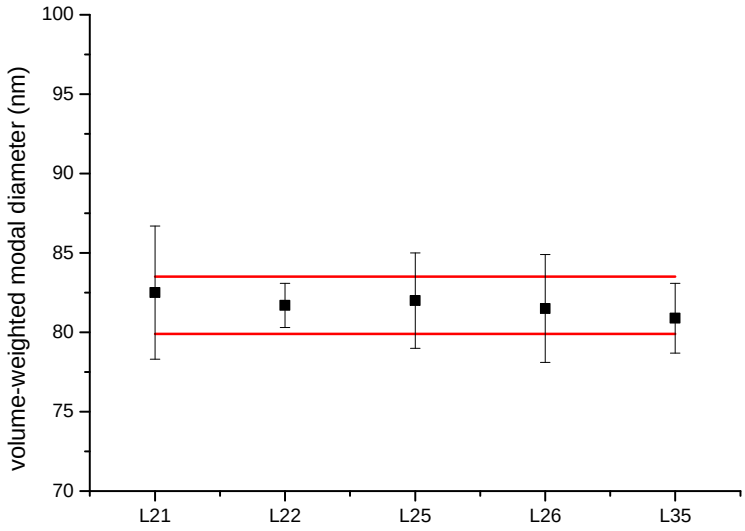

Fig. E5.3 Laboratory mean values of the volume-weighted-modal particle diameters as obtained by 5 laboratories using SAXS (model fitting approach). The error bars indicate the expanded (k = 2) measurement uncertainties as reported by the participants, the two horizontal lines reflect the certified range.

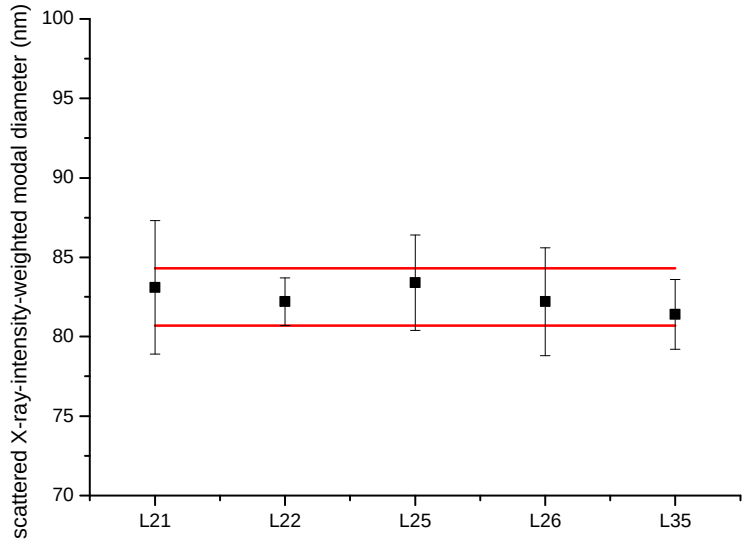

Fig. E5.4 Laboratory mean values of the scattered X-ray intensity-weighted-modal particle diameters as obtained by 5 laboratories using SAXS (model fitting approach). The error bars indicate the expanded (k = 2) measurement uncertainties as reported by the participants, the two horizontal lines reflect the certified range.

European Commission

EUR 28362 EN – Joint Research Centre – Directorate F – Health, Consumers and Reference Materials
Title: **CERTIFICATION REPORT The certification of equivalent diameters of silica nanoparticles in aqueous solution: ERM®-FD101b**
Author(s): Y. Ramaye, V. Kestens, A. Braun, T. Linsinger, A. Held, G. Roebben
Luxembourg: Publications Office of the European Union
2017 – 80 pp. – 21.0 x 29.7 cm
EUR – Scientific and Technical Research series – ISSN 1831-9424
ISBN 978-92-79-64637-9
doi: 10.2787/212519

As the Commission's in-house science service, the Joint Research Centre's mission is to provide EU policies with independent, evidence-based scientific and technical support throughout the whole policy cycle.

Working in close cooperation with policy Directorates-General, the JRC addresses key societal challenges while stimulating innovation through developing new methods, tools and standards, and sharing its know-how with the Member States, the scientific community and international partners.

Key policy areas include: environment and climate change; energy and transport; agriculture and food security; health and consumer protection; information society and digital agenda; safety and security, including nuclear; all supported through a cross-cutting and multi-disciplinary approach.

LA-NA-28362-EN-N

Publications Office

doi: 10.2787/212519

ISBN: 978-92-79-64637-9